ANALYSIS COVER SHEET

MECHANICAL ENG.
FILE NO: MISC 030-058 Rev A

PREPARED FOR PROGRAM: All	DATE: 20 June 1996
PREPARED BY: Tom Irvine	REVIEWED BY: Tom Irvine

ANALYSIS NAME: P95/50 Rule -- Theory and Application

OBJECTIVE:

The purpose of this report is to explain the P95/50 rule which is used for predicting maximum shock, vibration, and acoustic levels.

ASSUMPTIONS:

Statistical theory as given in the references.

RESULTS:

The P95/50 rule is explained by theory and example.

CONCLUSIONS:

The P95/50 rule can be used to predict maximum environmental levels. OSC engineers should use the tolerance factors from Reference 1 for this analysis.

REFERENCES:

1. C. Harris, editor, Shock and Vibration Handbook, Fourth Edition; A. Piersol, Chapter 20, "Test Criteria and Specifications," McGraw-Hill, New York, 1996.

2. H. Himelblau, et al, "Development of Cassini Acoustic Criteria Using Titan IV Flight Data," Draft of paper to be presented at IES ATM, May, 1992.

3. C. Eisenhart, M. Hastay, W. Wallis, editors, Selected Techniques of Statistical Analysis, Columbia University, McGraw-Hill, New York, 1947.

4. R. Walpole and R. Myers, Probability and Statistics for Engineers and Scientists, 2nd ed., Macmillan, New York, 1978.

5. G. Betteley, et al, Using Statistics in Industry, Prentice Hall, London, 1994.

IS ADDITIONAL ANALYSIS REQUIRED?	DESCRIBE:	COMPLETION DATE:
Optional	Revisions as needed.	20 June 1996

INTRODUCTION

An environmental test must *stimulate* and *simulate.*

An acceptance test, for example, must stimulate latent parts and workmanship defects. A qualification test must stimulate latent design flaws.

An environmental test must also simulate the expected flight conditions, to the extent possible.

This report is concerned with the simulation goal. It focuses on the statistical methods required for the prediction of maximum shock, vibration, and acoustics environments. Specific attention is given to the *Tolerance Limit Method.* The P95/50 rule is an application of this method.

BACKGROUND

The following paragraph is typical of guidelines given in MIL-STD-1540B and MIL-HDBK-340:

> The maximum predicted environment is defined as equal to or greater than the value at the ninety-fifth percentile value at least 50 percent of the time. Where there are less than three data samples, a minimum margin of 3 dB is applied to account for the variability of the environment.

Adding a 3 dB margin is straightforward. G values are simply multiplied by $\sqrt{2}$. G^2/Hz values are doubled.

The margin for *ninety-fifth percentile value at least 50 percent of the time*, however, is unclear. Note that P95/50 is an abbreviation for this guideline.

The remainder of this report will clarify the P95/50 rule.

THEORY

Tolerance Limit Basics

Again, the P95/50 rule is an application of the Tolerance Limit method.

A population of values may be described in terms of its mean μ and its standard deviation σ. The mean value is a measure of central tendency. The standard deviation is a measure of spread, or variation, about the mean.

A sample is a subset of a population. A particular rocket vehicle design may have a lifetime of 100 flights. The data from all flights would be the population. Data from three of the flights would be a sample of the population. The population mean and standard deviation values are unknown until the last flight has occurred. The corresponding sample values can be calculated after each flight, however.

The purpose of the Tolerance method is to estimate the variation in a population of values when only the sample mean and sample standard deviation values are known.

The Tolerance method assumes the following:

1. The population has a Normal distribution.
2. The samples are selected at random.

The sample mean $\bar{x}$ is defined as

$$\bar{x} = \frac{1}{n}\sum_{i=1}^{n} x_i \tag{1a}$$

where

n = number of samples,

x_i = individual sample values.

The sample standard deviation s is defined as

$$s = \sqrt{\frac{1}{(n-1)}\sum_{i=1}^{n}(x_i - \bar{x})^2} \tag{1b}$$

Upper Limit Approach

The Tolerance method can be applied in a number of ways. The *Upper Limit* form is the appropriate Tolerance approach for predicting maximum flight levels from flight or test data.

The problem is to find a tolerance factor k that will yield a limit which covers at least 100β percent of the population with a confidence of 100γ percent, as expressed by

$$P[\, F(\bar{x} + ks) \geq \beta] = \gamma \tag{2}$$

where F is a cumulative distribution function.

A Normal distribution of the population is assumed. Thus the cumulative distribution function represents the area under a Normal distribution, starting with $-\infty$.

The rest of this explanation is based on Piersol, Reference 1. A table from this reference is given in Appendix A. This approach is the same technique used in Himelblau, Reference 2. The complete Reference 2 paper is given in Appendix B.

An upper limit must be established using a tolerance factor k as follows

$$\text{Limit} = \bar{x} + ks \tag{3}$$

Note that the sample standard deviation is multiplied by k but that the sample mean is taken as is.

The tolerance factor k is a function of the number of samples n, the probability P, and the confidence limit γ. References 1 and 2 give brief tables for the tolerance factor based on these variables.

Tolerance Factor Calculation

Extrapolated Formula

References 1 and 2 are content to leave the reader with tables for the k value. Neither explains the theory behind the tables. Likewise, engineering statistical textbooks seem to indicate that a theoretical explanation is "beyond the scope" of the text.

Nevertheless, an understanding of the theory is necessary for intelligent use of the Upper Tolerance Limit method.

Reference 3 is largely a tabular source, but it also gives some theoretical explanation. It gives a double-sided approach, however, as opposed to the upper limit approach of interest in this report.

With some tentative extrapolation from Reference 3, the Upper Tolerance Limit Factor k is

$$k \approx \left\{ z \right\} \left\{ \sqrt{\frac{n-1}{\chi^2_\gamma}} \right\} \tag{4}$$

The variables in this equation are defined in the following sections.

Normal Distribution

The z value in Equation 4 is found from a Normal distribution curve. The z value is the ordinate corresponding to the probability area, as shown in Figure 1.

For example, the Normal distribution probability is 95% that a particular sample is less than or equal to a z value of 1.645, as shown in Reference 4. The *P95* in the *P95/50* rule thus comes from the Normal distribution.

Note that z is called the *standard deviate.* Also, note that

$$z = (x - \mu) / \sigma \qquad (5)$$

or

$$x = \mu + z\sigma \qquad (6)$$

Essentially, the Tolerance Limit method makes uses of this formula by replacing μ with $\bar{x}$, and σ with s. In other words, the population values are replaced with their corresponding sample values. Also, note the similarity between Equations 3 and 6.

Chi-square Distribution

The term in the second bracket set in Equation 4 comes from a Chi-square distribution. This distribution can be used to estimate a population standard deviation from a sample deviation. The χ^2_γ term is an ordinate which corresponds to some area under the Chi-square distribution curve. The area in this case represents a confidence value γ. Note that the *50* in *P95/50* corresponds to the confidence value. Note that the χ^2_γ term also depends on the number of degrees of freedom ν, where $\nu = n-1$.

Example:

Given that n=3 and $\gamma = 50\%$, find χ^2_γ.

$\nu = 2$,

$\chi^2_\gamma = 1.39$ from Reference 5.

Limiting Case

As the number of samples becomes large, the tolerance factor converges to the z value from the Normal distribution curve.

For example, the table in Appendix A shows that the tolerance factor k is equal to 1.64 for a 95% probability for an infinite number of samples, independent of the confidence value γ.

Note that

$$\lim_{n \to \infty} \left\{ \sqrt{\frac{n-1}{X_\gamma^2}} \right\} = 1 \tag{7}$$

Thus, the sample standard deviation approaches the population standard deviation as the number of samples becomes very large.

Check of Equation 4

An "approximately equal" sign is used for caution in Equation 4, since this exact formula is not explicitly given in any of the immediate references. Nevertheless, the formula can be verified by comparing its result for k with the tabular values in Reference 1. Three respective cases are given in Tables 1 through 3. Note that the Reference 1 tabular values are given in Appendix A.

Table 1. P95/50 for three samples, Tolerance Factor Calculation			
Description	Symbol	Value	Source
Samples	n	3	Given
Degrees-of-freedom	ν	2	$\nu = n-1$
Probability	P	95%	Given
Confidence	γ	50%	Given
z limit corresponding to P area in Normal Distribution curve	z	1.645	Reference 4
Chi-square value for ν and γ	x^2_γ	1.39	Reference 5
Calculated Tolerance Factor	k	1.97	Equation 4
Piersol Tolerance Factor	kp	1.94	Reference 1
Error between Tolerance Factors	(k - kp)/kp	+1.5%	—

Table 2. P99/90 for ten samples, Tolerance Factor Calculation			
Description	Symbol	Value	Source
Samples	n	10	Given
Degrees-of-freedom	ν	9	$\nu = n-1$
Probability	P	99%	Given
Confidence	γ	90%	Given
z limit corresponding to P area in Normal Distribution curve	z	2.33	Reference 4
Chi-square value for ν and γ	x^2_γ	4.17	Reference 5
Calculated Tolerance Factor	k	3.42	Equation 4
Piersol Tolerance Factor	kp	3.53	Reference 1
Error between Tolerance Factors	(k - kp)/kp	-3.1%	—

Table 3. P90/75 for seven samples, Tolerance Factor Calculation			
Description	Symbol	Value	Source
Samples	n	15	Given
Degrees-of-freedom	ν	14	$\nu = n-1$
Probability	P	90%	Given
Confidence	γ	75%	Given
z limit corresponding to P area in Normal Distribution curve	z	1.28	Reference 4
Chi-square value for ν and γ	χ^2_γ	10.17	Reference 5
Calculated Tolerance Factor	k	1.50	Equation 4
Piersol Tolerance Factor	kp	1.58	Reference 1
Error between Tolerance Factors	(k - kp)/kp	-4.9%	—

In each case, the tolerance value calculated via Equation 4 is within 5.0% of that from the tabular value in Reference 1. The difference may be due to round-off error, or possibly to the omission of some higher-order term in Equation 4.

For standardization, the tolerance values given in Reference 1 are recommended for use at OSC. Equation 4 is intended only for instructional purposes. Again, the Reference 1 values are given in Appendix A.

APPLICATION

An example was carried out via the follow steps:

1. A series of eight time histories were synthesized using a computer program.
2. Power spectral densities were calculated for each time history.
3. The sample average and sample standard deviation were calculated for each frequency.
4. A tolerance factor of k=1.73 was selected from the table in Appendix A, based on a P95/50 criteria for 8 samples.
5. The Upper Tolerance Limit approach was used to calculate a P95/50 Limit for each frequency, using the equation: $\text{Limit} = \overline{x} + ks$.

NORMAL DISTRIBUTION CURVE

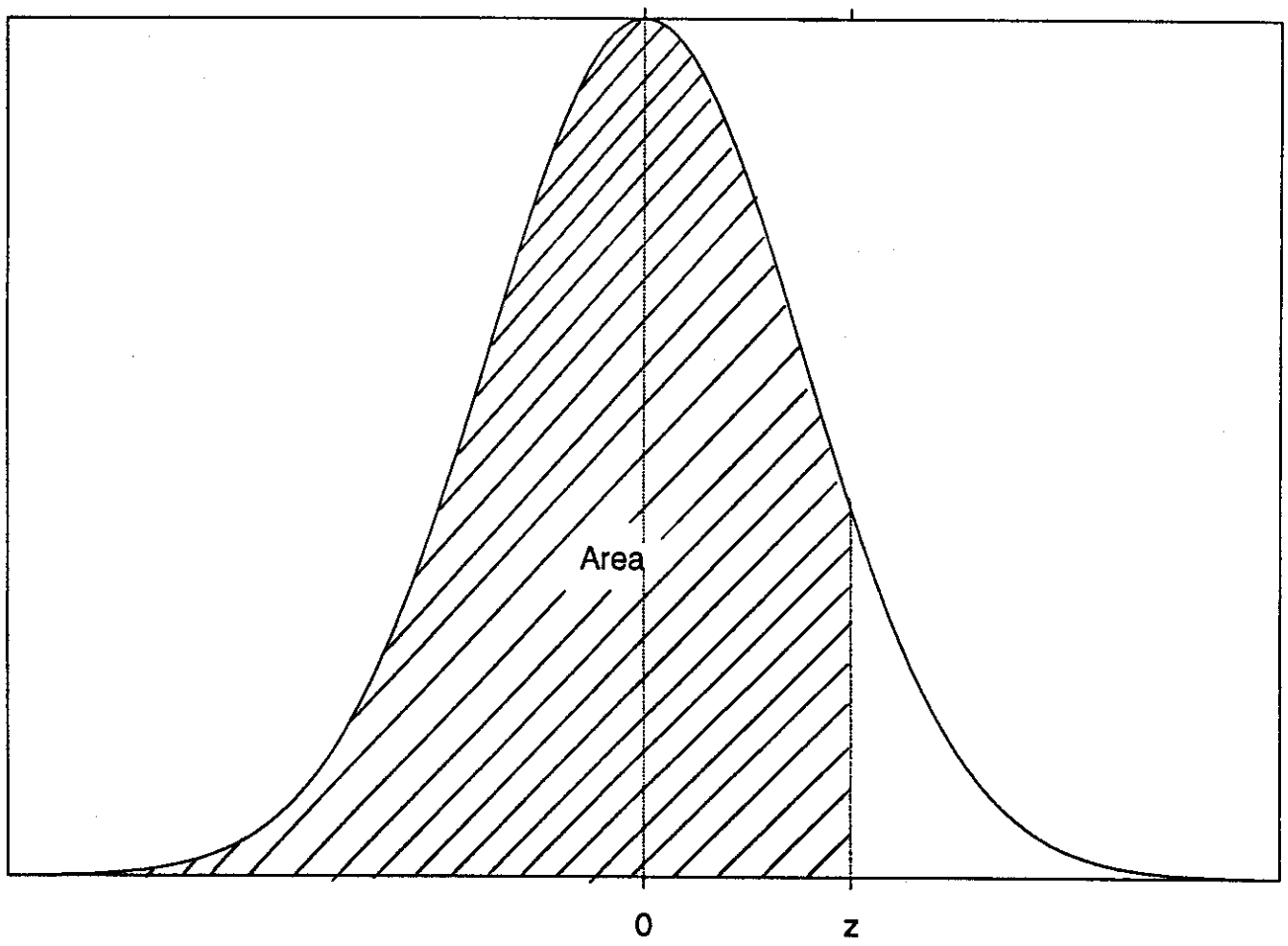

Figure 1.

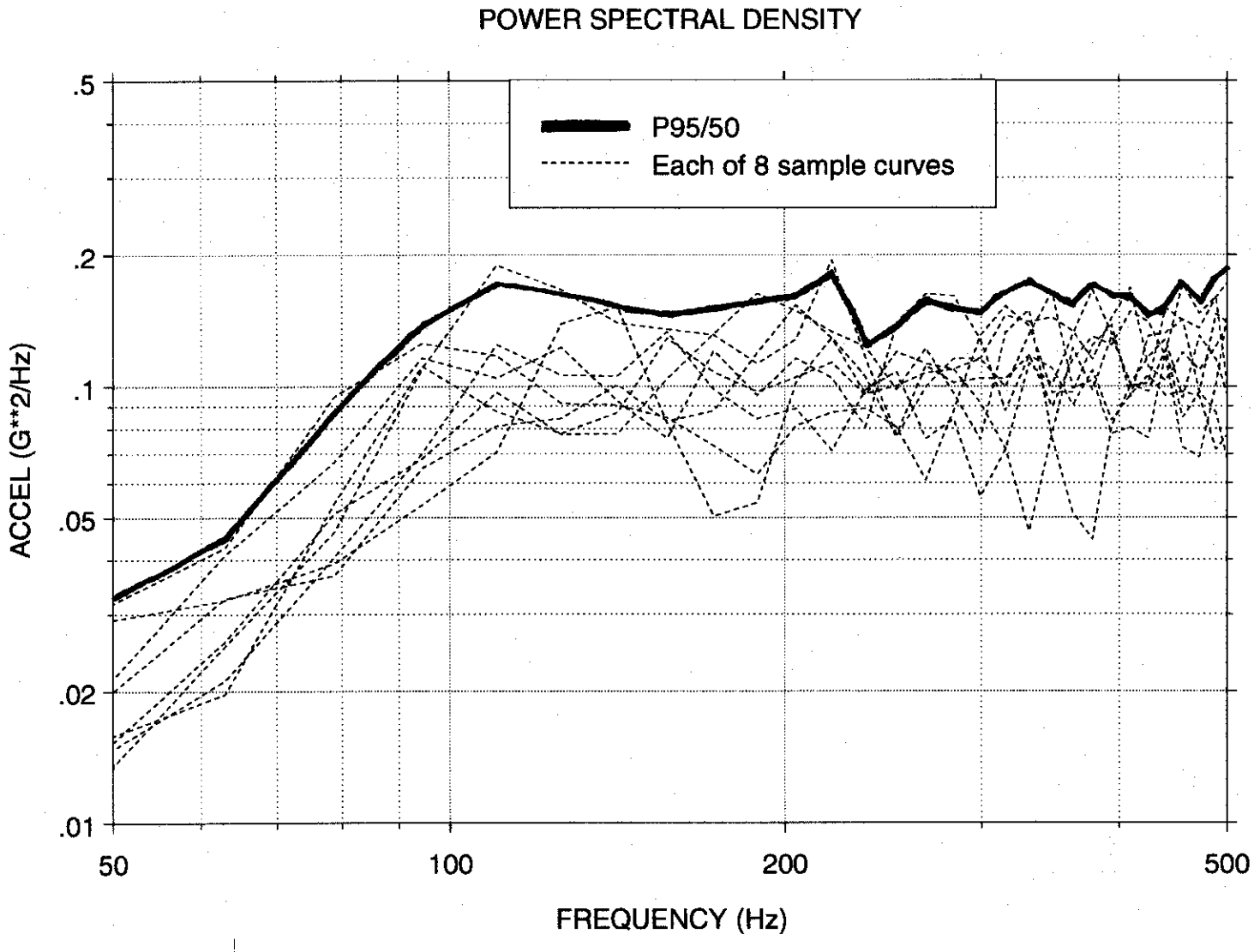
POWER SPECTRAL DENSITY
P95/50
Each of 8 sample curves
ACCEL (G**2/Hz)
.5
.2
.1
.05
.02
.01
50
100
200
500
FREQUENCY (Hz)

Figure 2.

Table IV. Statistical Tolerance Factors for Deriving Cassini 95/50% Acoustic Criteria Based on Number of Flight Measurements Analyzed (Reference 14)

Number	Tolerance Factor	Number	Tolerance Factor
2	2.339	16	1.678
3	1.939	17	1.676
4	1.830	18	1.674
5	1.779	19	1.673
6	1.750	20	1.671
7	1.732	21	1.670
8	1.719	22	1.669
9	1.709	23	1.668
10	1.702	24	1.667
11	1.696	25	1.666
12	1.691		
13	1.687	30	1.662
14	1.684	35	1.659
15	1.681	40	1.658
		45	1.656
		∞	1.64485

APPENDIX A

$$P[\,F(\bar{x}+ks) \geq \beta\,] = \gamma$$

TABLE 20.3 Normal Tolerance Factors for Upper Tolerance Limit, k values

	$\gamma = 0.50$			$\gamma = 0.75$			$\gamma = 0.90$		
n	$\beta = 0.90$	$\beta = 0.95$ *	$\beta = 0.99$	$\beta = 0.90$	$\beta = 0.95$	$\beta = 0.99$	$\beta = 0.90$	$\beta = 0.95$	$\beta = 0.99$
3	1.50	1.94	2.76	2.50	3.15	4.40	4.26	5.31	7.34
4	1.42	1.83	2.60	2.13	2.68	3.73	3.19	3.96	5.44
5	1.38	1.78	2.53	1.96	2.46	3.42	2.74	3.40	4.67
7	1.35	1.73	2.46	1.79	2.25	3.13	2.33	2.89	3.97
10	1.33	1.71	2.42	1.67	2.10	2.93	2.06	2.57	3.53
15	1.31	1.68	2.39	1.58	1.99	2.78	1.87	2.33	3.21
20	1.30	1.67	2.37	1.53	1.93	2.70	1.76	2.21	3.05
30	1.29	1.66	2.35	1.48	1.87	2.61	1.66	2.08	2.88
50	1.29	1.65	2.34	1.43	1.81	2.54	1.56	1.96	2.74
∞	1.28	1.64	2.33	1.28	1.64	2.33	1.28	1.64	2.33

* P95/50 column

This table is taken from Reference 1.

DEVELOPMENT OF CASSINI ACOUSTIC CRITERIA USING TITAN IV FLIGHT DATA

H. Himelblau, D. L. Kern, G. L. Davis
Mail Stop 301-456
Jet Propulsion Laboratory
California Institute of Technology
Pasadena, CA 91109-8099

Abstract

The Cassini spacecraft is being developed by the Jet Propulsion Laboratory (JPL) for the National Aeronautics and Space Administration (NASA) to orbit and explore the planet Saturn, its rings and satellites. Cassini will be launched on a Titan IV and boosted out of earth orbit by a Centaur. This paper discusses the development of Cassini acoustic criteria using Titan IV flight data. The Titan IV flight acoustic measurements and the different flight data processing techniques employed by Martin Marietta and The Aerospace Corporation are described and the implications discussed. The methods employed by JPL for identifying and correcting for instrumentation system transients are presented. Factors affecting the development of Cassini acoustic criteria using the corrected Titan IV flight data include the statistical methods used to account for spatial and flight-to-flight variations, the use of maximax spectra, data corrections for acoustic pressure increases near the payload fairing surfaces, and corrections for payload fill factor effects. Separate acoustic criteria were developed for different spacecraft zones, with resulting test implications.

Introduction

All major JPL spacecraft have been previously flight-qualified to acoustic noise (e.g., Reference 1), and for good reason: acoustic noise internal to the payload fairing (PLF) is the sole cause of the most severe random vibration experienced by these spacecraft (Reference 2). The Cassini spacecraft will be no exception. This spacecraft, shown in Figure 1, is to be launched on the recently-available Titan IV vehicle with new upgraded solid rocket motors (SRMs), and a Centaur upper stage. During the launch phase, Cassini and Centaur will be enclosed in a PLF comprised of isogrid aluminum construction, as shown in Figure 2 (Reference 3). Fortunately, a substantial number of acoustic measurements have been or will be made on the Titan IV, including the PLF. This measurement program has ended a twenty year hiatus since acoustic measurements were made last on Titan III. As summarized in Table I, there have been a total of 34 PLF acoustic measurements on the first four flights, specifically 10 external and 24 internal to the PLF. The internal measurements are obviously the most applicable to the Cassini acoustic design and test criteria. However, if anomalies or excessive internal flight-to-flight variations are observed, the external measurements should help to identify the cause.

The first two flights (K-1 and K-4) were launched from the Cape Canaveral AFS/Eastern Test Range (ETR), whereas the second two (K-5 and K-8) were launched from Vandenberg AFB/Western Test Range (WTR). The payload configurations, with and without upper stages, are different from Cassini/Centaur, which is to be launched from ETR. The Titan IVs for these flights used the standard SRMs. The new SRMs are still in development. In addition, there are some important differences in the launch pads and systems used, which will be discussed later.

Acoustical Blankets

Blankets, comprised of 3 in. thick fiberglass enclosed in glass fabric, were installed on portions of all four PLF interior surfaces. However, the amount of coverage varied from flight to flight, as described in Table II. The PLF used for Flight K-5 was 10 ft longer than the other three PLFs.

Microphone Installations and Locations

All of the microphones (mics) applicable to Cassini were attached to the PLF. Their locations are shown in Figures 3-6 (References 4-7). Although it would be greatly preferable to locate the mics directly on the spacecraft, managers are often reluctant to pass instrumentation cables through two disconnects (one between the spacecraft and upper stage, and the other between the upper stage and launch vehicle) to reach

To be presented to IES ATM May 1992

the telemetry transmitter in the launch vehicle. The potential consequences of a PLF/launch vehicle disconnect failure would obviously be much less critical. The external mics were attached to the interior of the PLF structure with their diaphragms protruding through holes to the external surface. The diaphragms were flush-mounted to properly measure aerodynamic noise while avoiding the disturbance of the aerodynamic flow field during periods of transonic flight and maximum dynamic pressure (max q). No protective caps were used on these mics. Thus great care was required to avoid diaphragm damage. Nineteen internal mics were internally attached to the PLF structure with diaphragms approximately 4 in. from the interior surface (between the isogrid stiffeners). Three K-4 and two K-8 internal microphones were installed on standoffs (or masts) approximately 20 in. from the PLF interior surface, as shown in Figure 7. All internal mics had protective caps. These standoff measurements provided a unique opportunity to observe the internal noise field away from the PLF surface, where the noise is generally less severe and more representative of the acoustic environment seen by the payload. Thus it would be expected that the Cassini spacecraft would be exposed to a lesser noise field than that indicated by data from the internal PLF surface mics. Since PLF vibration, excited by external SRM exhaust-induced acoustic noise at liftoff, or flow-induced aerodynamic noise at transonic/max q, generates the internal noise (Reference 2), the noise emanating from the PLF surface is greater near the source (the direct field) than in the remaining space (the semi-reverberant field).

The internal mics, PCB Models 106M59 or 106M79, and external mics, PCB Model 106M80, were installed by McDonnell Douglas, the PLF supplier. These mics were not vibration-compensated, but were individually tested for vibration sensitivity. The remainder of the system was part of the Wideband Instrumentation System (WIS), supplied by Martin Marietta Corporation (MMC), developer of the Titan IV. Many other measurements throughout the vehicle, including vibration, were made via the WIS.

Acoustic Data Processing

All the acoustic signals were recorded on magnetic tape at either the ETR or WTR after telemetry reception. Tape dubs were subsequently made. Two organizations, MMC and The Aerospace Corporation (TAC) (the latter as technical advisors to the Air Force Space System Division), performed further data processing and analysis in a conscientious and straight-forward manner. As a result, it was unnecessary for JPL to reprocess or reanalyze the data. Nevertheless, some instrumentation problems were encountered. Figures 8 and 9 show instantaneous acoustic pressure histories of the same wideband liftoff data recorded at two different telemetry receiver sites (Reference 5). Many high-magnitude short-duration instrumentation system transients, sometimes called telemetry drop-outs, are observed in Figure 8, especially from T+0 (SRM ignition) to T+4 sec. Much better results are observed in Figure 9, where these transients occur only at T+1.7, T+1.9, T+3.2 and, as later found, at T+4.3 sec. With the aid of Butterworth plots from TAC, JPL was able to deal successfully with occasional instrumentation transients.

Butterworth plots are really rms pressure histories, which may be either overall (OA) or filtered in 1/3 octave bands (1/3 OBs), with a user-selectable linear averaging time. The rms values are then converted to either OA or 1/3 OB sound pressure levels (SPLs). The Butterworth plots furnished by TAC used a very short averaging time of T_{av} = 0.1 sec. This averaging time was clearly insufficient to permit the accurate computation of SPL, due to excessive random error, except for the OA or for higher frequencies. However, the short averaging time was ideal for determining if the instrumentation transients affected the SPLs. Three examples from Measurement 9737 of Flight K-4 are shown in Figures 10-12. The Butterworth plot of Figure 10 shows that the transients at T+1.7 and T+4.3 sec significantly influence the OA SPL history, whereas the transients at T+1.9 and T+3.2 sec do not. Figure 11 shows that none of the transients affected the 1/3 OB SPL history at a center frequency of 100 Hz. However, Figure 12 shows that only the transient at T+4.3 sec does not influence the 1/3 OB SPL history at 2.5 kHz. Armed with these plots, JPL was later able to remove any acoustic data contaminated with transients. Unfortunately, JPL also found that there was no trend in transient contamination, requiring that all 850 Butterworth plots be manually examined to successfully deal with the problem.

The instrumentation system background noise floor can also be observed in Figure 8-12 before liftoff (i.e., before T+0 sec). When the pressure signal is low, a signal-to-noise (S/N) problem is encountered, especially when S/N is less than 6dB. For example, Figure 12 shows a maximum S/N of 4dB, requiring a correction to remove the effects of the background noise. When S/N is 3dB or less, no accurate correction is possible. The data must be discarded when this occurs.

After dealing with instrumentation noise sources, it is then possible to concentrate on the acoustic data itself.

JPL was fortunate to have four thorough data sources in the form of MMC flight test reports (References 4-7). Data from these reports showed that the most severe internal acoustic environment occurred during liftoff, rather than during transonic flight or max q, even though the maximum external environment occurred during transonic flight over portions of the PLF aft of the cone-cylinder junction (CCJ), located at PLF Sta. 552 in Figure 2. [There are four possible causes of this apparent contradiction: (a) lower static pressure inside the PLF during transonic/max q, due to venting of the PLF to reduce structural loads, (b) the spatial-average external rms pressure over the PLF during transonic/max q was less than during liftoff, even though the local maximum rms pressure was greater, (c) critical PLF structural modes were not driven as well at transonic/max q as they were at liftoff, and (d) increased system damping of the PLF structure due to external aeroelastic interaction, as first demonstrated in Reference 8. This contradiction was identified as early as the Saturn/Apollo program. Reference 9 simply refers to the attenuation provided by (b) through (d) as "coupling inefficiency".] There can be an important exception to the conclusion that liftoff internal acoustics is generally more severe. High narrowband noise has been observed near payload vents during transonic/max q, e.g., inside the Shuttle payload bay near 300Hz on some flights and inside a Commercial Titan PLF on one flight near 900Hz. However, no PLF vent noise was observed during the first four Titan IV flights, even though the mics were close enough to the 12 vents (at PLF Sta. 148 for Flights K-1 and K-5, and Sta. 188 for K-4 and K-8) to measure any vent noise existing. It is currently anticipated that vent noise need not be considered for the Cassini spacecraft.

Derivation of Maximax Spectra

To derive Cassini acoustic criteria, JPL was specifically interested in obtaining the maximum SPL in each 1/3 OB for all the internal PLF acoustic measurements. These various maxima do not occur at the same instant of time, but at various intervals during the liftoff event due to the nonstationary character of the external SRM-induced noise field. However, it is currently impractical to design or test a structure to short-duration time-varying (i.e., nonstationary) loading. To avoid underdesign or undertesting, the maximum SPLs are used to establish a maximax spectrum, to be applied simultaneously to the structure as a time-limited stationary loading.

The various maximum SPLs were obtained from References 4-7. Taking one microphone (Meas. 9725) and flight (K-1) for example, the last column of Table III from Reference 4 shows the maximum 1/3 OB SPLs for each of the 1/3 OB center frequencies shown in the first column. Because of the substantial amount of data to be processed for each flight, it was impossible within the specified schedule for MMC personnel to determine which of the maximum 1/3 OB SPLs were contaminated by instrumentation transients. Because of the importance of using uncontaminated data in deriving Cassini criteria, JPL personnel performed this task with the aid of the Butterworth plots described previously.

Instrumentation Contamination Removal Procedure

In additional to showing the maximum 1/3 OB SPLs, Table III also shows the 1/3 OB SPL histories for the complete liftoff event from T+0 through T+8 sec. In particular, for each 1/3 OB center frequency listed in the first column, Table III shows the 1/3 OB SPL for the 1 sec time interval (or slice) from T+0 to T+1 sec, T+0.5 to T+1.5 sec, T+1 to T+2 sec, etc. until T+7 to T+8 sec is reached, using a linear average with a conventional averaging time T_{av} of 1 sec. This presentation is referred to as stepwise linear averaging with 50% overlap, with the amount of overlap considered acceptable based on the rate of level change during liftoff. If JPL personnel found that transient contamination (as noted from the applicable Butterworth plot) occurred during the time interval that the 1/3 OB SPL was maximum, then the next highest 1/3 OB SPL interval was selected unless contamination was again observed. If necessary, this procedure was repeated until the highest uncontaminated level was determined.

Once each uncontaminated maximum 1/3 OB SPL was determined across the frequency range, these were labeled as the maximax spectrum for that measurement and flight. As previously mentioned, these maxima occurred at various time intervals. The maximax label was given to avoid confusion with the maximum OA SPL and its 1/3 OB spectrum, the latter of course occurring at the same time interval as the maximum OA SPL. (Note that Table III did not identify the maximum OA SPL or its time interval.) Incidently, there was no observed relationship of the time of occurrence of each maximum 1/3 OB SPL with frequency.

A study was recently performed on Titan IV and Shuttle liftoff internal PLF acoustic data to determine the optimum averaging times to be used for 1/3 OB analysis (Reference 10). It was concluded that the Titan IV optimum averaging times should be T_o = 1.14 sec for the OA SPL, and $T_{oi} = 4.88/f_i^{0.2}$ for 1/3 OB SPLs,

where f_i is the applicable 1/3 OB center frequency. However, it was pointed out that the total rms error would be within 25% of the minimum if (a) T_{av} = 1 sec were used for the overall and 1/3 OB center frequencies greater than 250Hz, and (b) T_{av} = 2 sec for center frequencies equal to or less than 250Hz. Unfortunately, since the receipt of this study, there was insufficient time to reanalyze all the internal PLF acoustic data at and below 250Hz, as recommended. Thus all maximax spectra presented here were derived using the conventional T_{av} = 1 sec.

Uncontaminated liftoff maximax spectra for all 19 internal acoustic measurements made during the first four Titan IV flights are shown in Figures 13-18. Similar spectra for the ten external measurements are shown in Figures 19-20.

Fill Factor Effects

It has been previously observed that the internal acoustic environment is usually higher when the distance from the PLF to the payload surface is short. Based on measured Shuttle flight data, Reference 11 developed a graph shown in Figure 21 for predicting 1/3 OB SPL increases for decreasing distances. Since the flight data had substantial scatter, a certain amount of conservatism was used in the prediction. This graph was later modified to enable its application to conventional payloads on expendable launch vehicles (ELVs), such as Titan IV. Subsequently Reference 12 developed an improved graph for conventional ELV payloads, shown in Figure 22, based on statistical energy analysis, which removed the unnecessary conservatism and can therefore be used for either increasing or decreasing PLF-to-payload surface distances. (However, some care may need to be taken in certain applications.) During Flight K-5, Meas. 9705, 9706 and 9707 were located where the PLF-to-payload surface distances were 34, 40 and 25 in., respectively. During Flight K-8, Meas. 9715, 9716 and 9717 were located where the distance was 25 in. in all three cases. In order to remove these fill factor effects from subsequent acoustic criteria development, the 1/3 OB SPLs for these measurements (shown in Figures 16 and 17) were reduced using Figure 22. These inverse fill factor-adjusted maximax spectra are shown in Figures 23 and 24. As a result, all 19 internal PLF acoustic spectra may now be treated on an equal weight basis.

Selection of Acoustic Criteria

Comparison of Figures 13, 14, 23 and 24 shows that there is significant scatter in the maximax acoustic spectra from the 19 internal PLF surface measurements, caused by flight-to-flight as well as spatial variations. Under these circumstances, it is conventional to perform a statistical analysis of the data population, determine or assume a statistical distribution, and select a criteria based on a given probability and confidence of not exceeding the resulting criteria. JPL personnel decided to select the acoustic criteria based on the recommendations in Reference 13; namely, assume the population is normally distributed, determine the mean and standard deviation of the population, and compute the resulting criteria based on a 95% probability of not exceeding the criteria with a 50% confidence.

This analysis may be expressed mathematically as $x_{cr} = \bar{x} + k\, s_x$, where x_{cr}, $\bar{x}$ and s_x are the criteria, mean value and standard deviation of the population, and k is the tolerance factor. The value of the tolerance factor is a function of the probability and confidence selected, and the number of samples. Table IV from Reference 14 shows this factor as a function of the number of samples for a 95/50% tolerance statement. It should be noted that only Reference 14 provides values of k for a wide range of probabilities and tolerances, whereas other references (including Reference 15) have only a limited range available and do not include the 95/50% tolerance. Incidently, it has traditionally been found that the 95/50% criteria roughly approximates the data envelope when more than just a few measurements are made. The data and envelope of the 19 inverse fill factor-adjusted internal PLF surface maximax acoustic spectra are shown in Figure 25.

Figure 26 shows the mean and 95/50% criteria for the above 19 spectra, along with the envelope and the current Cassini flight acceptance (FA) criteria. It is seen that the envelope exceeds the current FA criteria, although the 95/50% criteria does not. Examination of Figures 13, 14, 23 and 24 shows that all the exceedances occurred during Flight K-8; specifically Meas. 9715FF and 9717FF at 25Hz, Meas. 9716FF at 31.5Hz, Meas. 9709 at 160 and 200Hz, and Meas. 9705 between 125 and 315Hz. Based on the 95/50% criteria for the 19 spectra, no change to the current FA criteria is necessary. However, there is considerable concern about the exceedances, especially the 4dB at 200 Hz from Meas. 9705 of Flight K-8. This is especially troubling when Meas. 9705 from Flight K-8 is compared with a similar Meas. 9705 from Flight K-5, illustrated in Figure 27, which shows that the K-8 spectrum exceeds the K-5 spectrum by 7dB at 200Hz. (These measurements are in similar, but not identical locations, as the K-5 PLF is 10 ft longer than the K-8 PLF.) In addition, there is a general concern about the significant flight-to-flight variations in the acoustic spectra, causing

a re-evaluation of the assumption that the data should be treated as a single population.

Launch Pad Effects

It is readily observable that the spectra in Figures 13 and 14 from Flights K-1 and K-4, launched from the ETR, are significantly lower than the spectra in Figures 23 and 24 from Flights K-5 and K-8, launched from the WTR. If there are important differences between ETR and WTR launch pad configurations and conditions affecting the acoustic noise generated by the SRMs, this could have a beneficial effect on the Cassini acoustic criteria, since the spacecraft is to be launched from the ETR. For example, Figure 28 shows that the 95/50% criteria and envelope for the 8 internal PLF surface measurements from Flights K-1 and K-4 are significantly less than the current Cassini FA criteria, whereas Figure 29 shows that the 95/50% criteria for the 11 corresponding measurements from Flights K-5 and K-8 slightly exceed the current Cassini criteria at 25 and 250Hz. In addition, a comparison of overall pressure histories from ETR and WTR show a different character of the data, as illustrated in Figure 30 from Reference 10.

Examination of the ETR and WTR launch pads shows that there are many similarities and some differences, as indicated in Figure 31. In both cases, the SRM exhaust flows are directed into a single covered launch duct, whose length is approximately 135 ft and whose relative cross sectional areas are approximately the same. On Flight K-1, a significant low frequency overpressure (O/P) transient, which propagated up the vehicle at the speed of sound, was generated at SRM ignition. To attenuate this transient, O/P water suppression systems were installed at both facilities. As a result, the O/P was substantially reduced for the following three flights. Both systems were designed to achieve their maximum water flow rates from about T-1.5 to T+4 sec, with water valve shutoff at T+6 sec. Thus some effect on liftoff noise should have been observed. However, the maximum flow rates were considerably different: 50,000 gpm of water was applied to the SRM exhaust flows at the exhaust duct inlet at the ETR, whereas 60,000 gpm was applied at the inlet and an additional 25,000 gpm at the duct exit at the WTR. Thus, if water did attenuate liftoff acoustics prior to T+4 sec, as well as the O/P transient, then greater attenuation should have been achieved at the WTR. This hypothesis is in obvious contradiction to the observed acoustic increase at the WTR. The effects of the different Umbilical Towers are currently being investigated.

After T+3 sec, the increasing vehicle altitude above the launch pad is high enough for most of the diverging SRM exhaust flows to impact the top of the pad rather than enter the duct, so that water attenuation would no longer be effective. This is confirmed by the OA SPL history of Meas. 9705 from Flight K-5, but is in contradiction to the history of Meas. 9737 from Flight K-4, both of which are shown in Figure 30.

Status of Acoustic Criteria

Until more data becomes available, it is unlikely that the acoustical differences between the ETR and WTR will be resolved. Meanwhile, JPL personnel recommend no change to the current Cassini acoustic criteria. It should be noted that most of the spacecraft will be exposed to an acoustic environment less than that indicated in Figure 26, because the 19 internal measurements used for developing the 95/50% criteria were located adjacent to the PLF surface. The spectral differences between the average of the 6 measurements made at the PLF surface and that of the 3 measurements made at the 20 in. standoffs during Flight K-4 are shown in Figure 32. Similarly, the average differences between the 8 surface and 2 standoff measurements during Flight K-8 are shown in Figure 33. Applying these differences to the exceedances shown in Figure 29 indicates that the spacecraft will not be exposed to an acoustic environment greater than the current Cassini criteria.

Two Cassini assemblies are close enough to the PLF surface that exceedances of the basic FA acoustic criteria are anticipated. Specifically, they are the Huygens Probe (HP), located at a PLF-to-HP distance of 21.5 in., and the Turntable Sunshade (SS), located at a PLF-to-SS distance of 11.5 in. The Huygens Probe (shown in the left rear of the spacecraft in Figure 1 and in the right center in Figure 2) is a separate spacecraft designed to parachute and land on Titan, the largest Saturn satellite. The Sunshade (shown in the right rear in Figure 1 and in the lower center in Figure 2) protects the Turntable and its several scientific instruments. Flight acceptance (FA) acoustic criteria were derived for these assemblies based on the direct application of the fill factor shown in Figure 22. All three Cassini FA acoustic criteria are shown in Figure 34, along with the current launch vehicle interface requirement of Reference 16, which needs to be updated. In addition, a vibroacoustic analysis will be performed to determine the loading on the Cassini antenna, which separates the upper and lower portions of the payload cavity at PLF Sta. 552, as observed in Figure 2. JPL traditionally sets design and qual test criteria at 4dB above the FA criteria. These criteria are shown in Figure 35. When

acoustic testing is performed later in the program, it is anticipated that the Huygens Probe, and the Turntable, assemblies, and Sunshade, will be tested separately to the higher criteria. Consideration will also need to be given as to whether local "hot spot" horns will be required to excite these hardware to the higher criteria during the spacecraft system acoustic test.

Acknowledgements

There are so many contributors to this document that it is impractical to list them all. However, the authors would be remiss not to mention the following individuals for their unique contributions: Mr. A. R. Hoffman of JPL, Ms. L. Bradford of MMC, Ms. C. S. Tanner and L. O. Crosse of TAC, and Mr. A. G. Piersol of Piersol Engineering Corporation. The research described in this paper was carried out at the Jet Propulsion Laboratory, California Institute of Technology, under a contract with the National Aeronautics and Space Administration.

References:

1. Hoffman, A. R., "Galileo Environmental Test and Analysis Program Summary," Proc., 13th Aerospace Testing Seminar, pp. 185-202, Oct. 1991.

2. Himelblau, H., Fuller, C. M. and Scharton, T. D., "Assessment of Space Vehicle Aeroacoustically-Induced Vibration Prediction, Design, Analysis and Testing," NASA CR-1596, July 1970.

3. Anon., "Titan IV System to Space Vehicle System Interface Control Document," MMC Doc. ICD-TIV/SV-24027, Feb. 1992.

4. Bradford, L. and Salem, L., "Titan IV-01 Flight Report, Wideband Instrumentation System (WIS) High Frequency Channels," Martin Marietta Rep. MCR-90-2702, Mar. 15, 1991.

5. Bradford, L. and Salem, L., "Payload Fairing Acoustic Data (Titan IV-04)," Martin Marietta Rep. MCR-XX-XXXX, Sept. 1990.

6. Bradford, L. and Salem, L., "Titan IV-05 Flight Report, Wideband Instrumentation System (WIS) High Frequency Channels," Martin Marietta Rep. MCR-91-2591, May 15, 1991.

7. Bradford, L. and Boone, A., "Titan IV-08 Flight Report, Wideband Instrumentation System (WIS) Acoustic Data," Martin Marietta Rep. MCR-91-2771, Mar. 1992.

8. Muhlstein, L., "Experimental Evaluation of the Aerodynamic Damping of Skin Panels at Low Supersonic Mach Numbers," AIAA Paper 72-402, Apr. 1972.

9. Elliott, K. E., "Titan Vibroacoustics," ELV Payload Environment (Lauriente, M. and Hoegy, H., Ed.), Chap. 11, University Research Foundation, 1990.

10. Piersol, A. G., "Optimum Data Analysis Procedures for Titan IV and Space Shuttle Payload Acoustic Measurement during Lift-Off," JPL Subcontractor Rep. 99501365, Dec. 23, 1991.

11. Tanner, C. S., "Acoustic Environments for DOD Payloads on Shuttle," Proc., Shuttle Payload Dynamic Environments and Loads Prediction Workshop, JPL Doc. D-1347, Vol. I, pp. 231-251, Jan. 1984.

12. Manning, J. E., "Analysis and Evaluation of the Fill Factor," Cambridge Collaborative Rep. 91-6-12104-1, Jan. 28, 1991.

13. Anon., "Military Standard: Test Requirements for Space Vehicles," MIL-STD-1540B (USAF), Rev. (Notice 3) Feb. 12, 1991.

14. Owen, D. B., "Factors for One-Sided Tolerance Limits and for Variables Sampling Plans," Sandia Monograph SCR-607, Mar. 1963.

15. Owen, D. B., Handbook of Statistical Tables, Addison-Wesley Pub. Co., Reading, MA, 1962.

16. Anon., "Cassini Launch Vehicle Requirements," JPL Doc. 699-020-2, Rev. Feb. 20, 1992.

For infinite No of Samples

Tolerance = 1.6448

Table I. Number of Titan IV Flight Measurements Used to Derive Cassini Acoustic Criteria

Launch Site	Flight	External	Internal		Fill Factor Affected
			PLF Surface	Standoff	
ETR	K-1	1	2	0	0
	K-4	4	6	3	0
WTR	K-5	0	3	0	3
	K-8	5	8	2	3

Table II. Extent of Payload Fairing Blanket Coverage Utilized on First Four Titan IV Flights (References 4-7)

Flight	PLF Station	
	Lower	Upper
K-1	156	432
K-4	52	432
K-5	52	701
K-8	52	432

Table III. 1/3 Octave Band Sound Pressure Level Histories Using Stepwise Linear Averaging with an Averaging Time of 1 Second and 50 Percent Overlap for Flight K-1 Measurement 9725 During Liftoff, Plus the Maximum Level for Each 1/3 Octave-Band Center Frequency (Reference 4)

Start time: / Freq (Hz)	0.0 (dB)	0.5 (dB)	1.0 (dB)	1.5 (dB)	2.0 (dB)	2.5 (dB)	3.0 (dB)	3.5 (dB)	4.0 (dB)	4.5 (dB)	5.0 (dB)	5.5 (dB)	6.0 (dB)	6.5 (dB)	7.0 (dB)	Max Env (dB)
20	105.7	105.4	103.7	99.9	101.5	103.7	101.4	103.7	105.2	109.1	109.4	111.7	109.9	102.8	103.8	111.7
25	114.3	116.0	107.1	105.0	105.8	106.4	107.1	106.3	107.9	109.6	110.3	109.7	100.8	105.4	106.7	116.0
31	131.3	129.5	119.5	116.8	120.0	120.3	115.9	114.5	115.1	116.1	115.8	114.5	113.5	110.3	113.3	131.3
39	128.1	127.0	122.3	119.5	115.9	116.4	115.5	112.5	114.1	116.9	110.2	110.5	110.7	115.3	114.0	128.1
50	121.5	121.8	113.7	111.4	112.7	114.0	113.0	112.4	115.0	119.0	110.7	115.8	117.0	117.5	114.7	121.8
62	125.2	125.0	116.8	116.0	113.4	113.9	114.9	116.7	118.4	119.2	117.7	118.4	117.5	116.6	116.5	125.2
79	125.9	126.0	116.2	117.0	116.4	113.7	115.6	114.3	115.6	117.6	117.9	110.6	117.0	115.7	113.6	126.0
99	122.0	121.8	117.3	116.0	116.4	117.6	118.0	117.9	119.5	122.3	122.2	120.6	120.0	118.1	116.2	122.3
125	122.2	122.1	118.0	117.1	117.5	117.7	118.2	121.0	122.0	122.6	122.2	121.2	119.3	117.9	115.0	122.0
157	120.0	120.2	117.7	116.6	118.1	119.5	119.8	120.2	120.6	120.4	120.2	120.5	118.6	116.2	112.4	120.6
198	118.1	118.8	118.8	118.1	118.5	119.1	120.5	120.3	119.8	121.6	120.6	118.6	117.4	114.7	111.5	121.6
250	120.3	119.0	119.2	120.7	122.3	123.6	124.6	124.0	123.5	122.6	122.5	122.0	120.4	116.8	113.5	124.6
315	119.5	117.2	120.4	123.1	124.5	125.5	126.1	125.0	122.6	123.2	123.0	121.3	119.9	117.2	114.3	126.1
397	116.7	116.3	118.4	120.6	123.3	123.0	121.7	122.1	121.7	121.2	119.7	118.5	117.0	114.1	109.6	123.3
500	114.1	113.5	115.9	117.9	120.1	120.6	120.0	119.1	118.6	117.9	117.3	115.9	112.9	109.6	106.6	120.6
630	111.9	112.4	116.5	116.8	118.3	118.5	117.7	117.5	117.0	116.6	115.8	114.6	112.4	108.7	105.0	118.5
794	110.6	110.8	112.7	115.6	116.9	117.4	117.0	116.2	115.9	115.3	114.1	112.8	111.1	108.8	106.7	117.4
1000	109.0	108.1	112.3	114.4	115.3	115.8	115.5	115.1	114.3	113.4	112.5	110.8	108.8	105.2	101.8	115.8
1260	105.3	104.5	108.5	110.5	111.3	111.7	111.3	110.8	110.3	109.4	107.9	106.7	104.6	101.4	98.9	111.7
1587	106.4	105.1	107.8	109.6	110.6	110.7	110.3	110.0	109.5	109.0	107.8	106.0	104.0	101.5	99.4	110.7
2000	106.7	106.5	109.6	111.3	112.3	113.2	113.2	112.5	111.6	110.4	108.8	107.0	104.6	102.4	100.3	113.2
2520	104.4	103.4	106.0	107.3	108.4	109.0	109.6	107.8	107.1	106.6	105.1	103.3	101.8	100.1	99.0	109.6
3175	102.8	102.3	105.5	106.0	106.5	107.0	105.3	104.7	104.3	103.9	103.3	102.5	101.6	100.6	100.2	107.0
4000	103.2	104.1	108.8	108.8	106.5	106.9	106.8	105.7	105.0	104.6	103.9	103.0	102.2	101.6	101.6	108.8

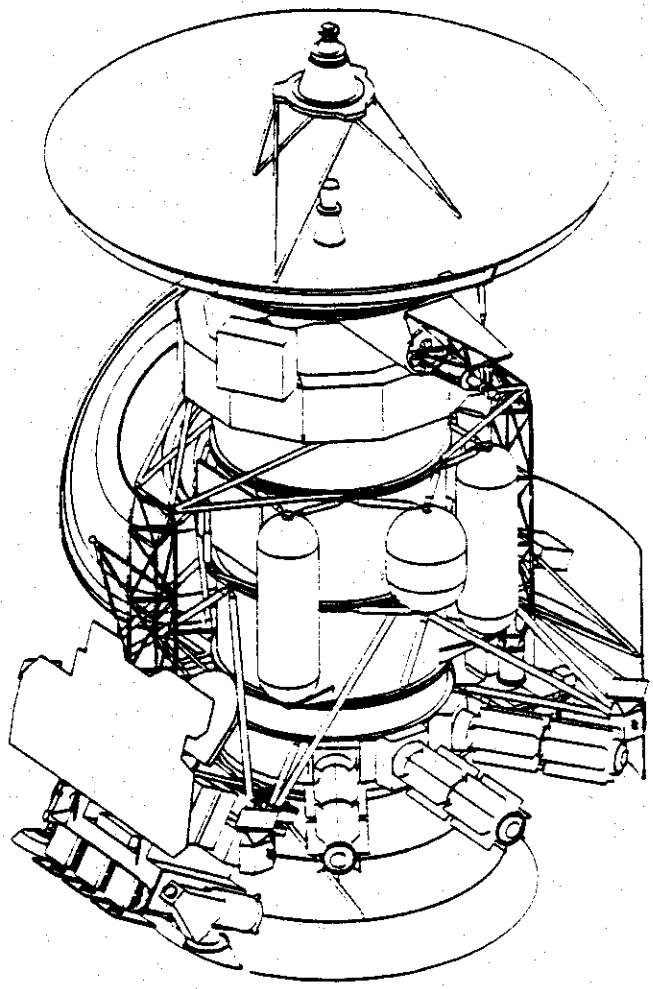

Figure 1. Trimetric View of the Cassini Spacecraft in its Launch Configuration

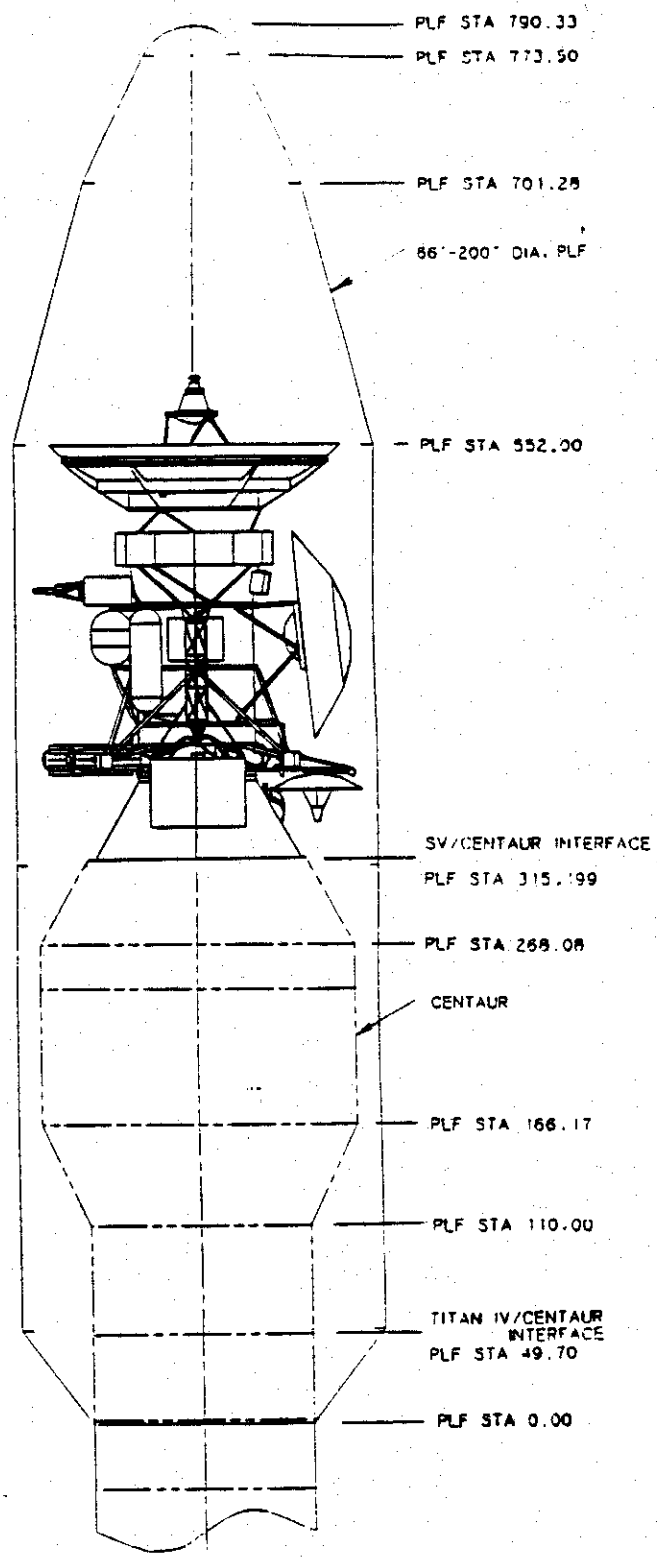

Figure 2. Installation of the Cassini Spacecraft and Centaur Upper Stage in the Titan IV Payload Fairing

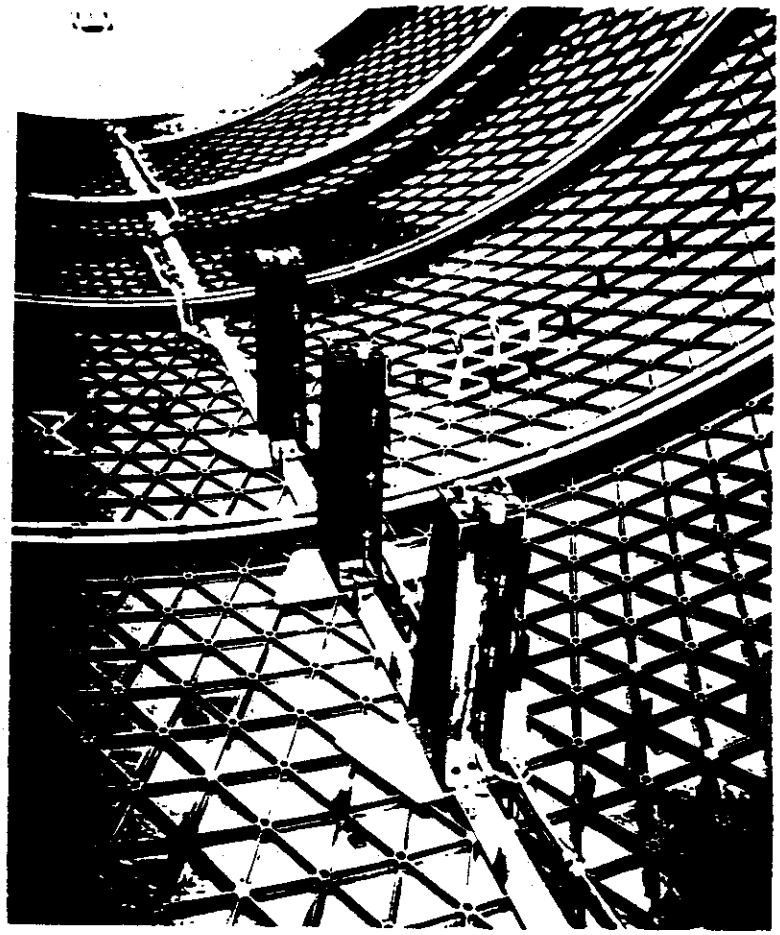

Figure 7. Installation of Microphones on Standoffs Supported by the Titan IV Isogrid Payload Fairing (Reference 5)

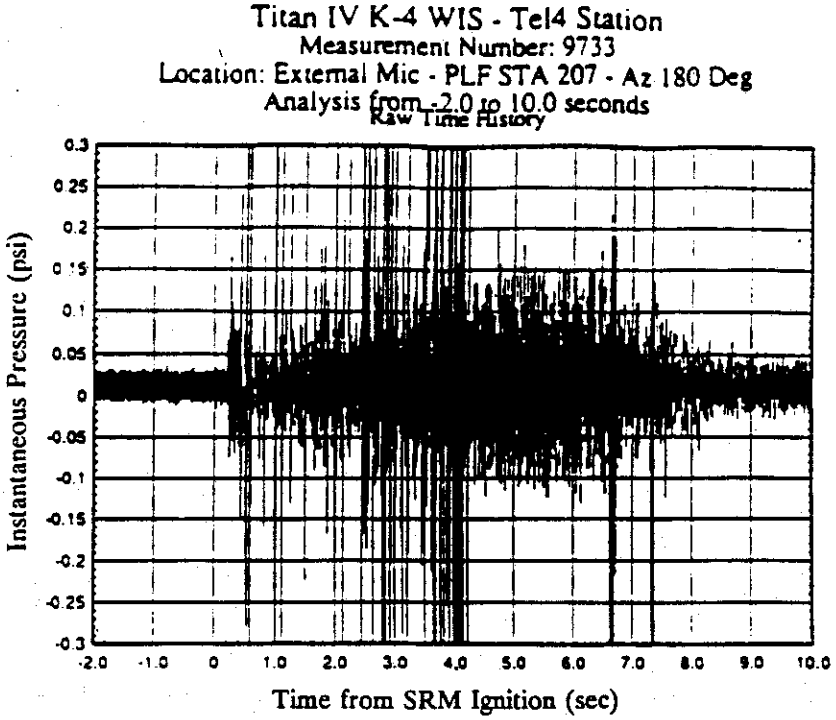

Figure 8. Wideband Instantaneous Pressure History Showing Instrumentation System Transients Due to Poor Telemetry Reception at Liftoff (Reference 5)

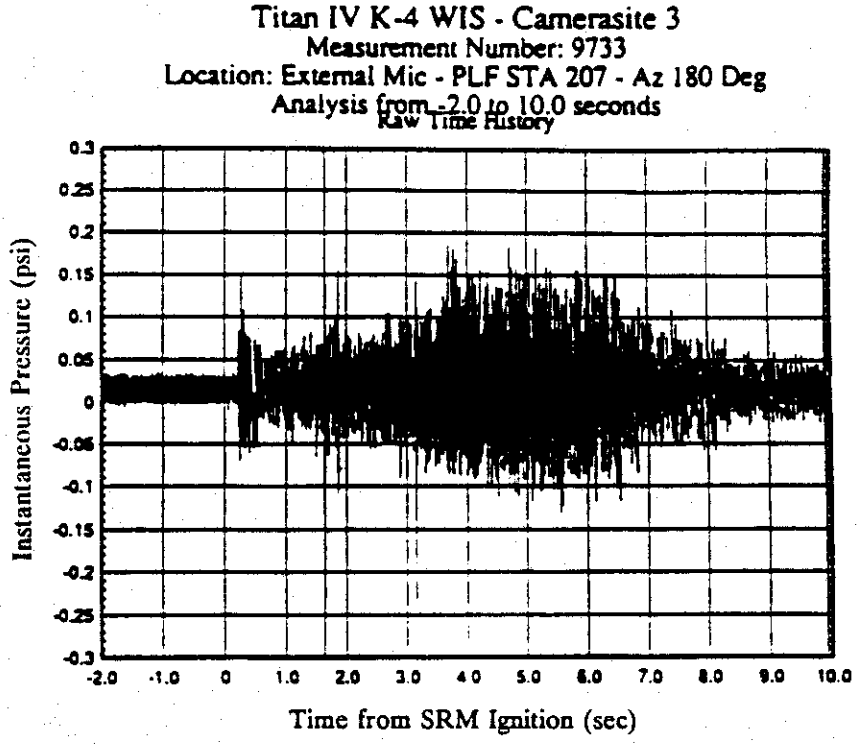

Figure 9. Wideband Instantaneous Pressure History Showing Instrumentation System Transients Due to Improved Telemetry Reception at Liftoff (Reference 5)

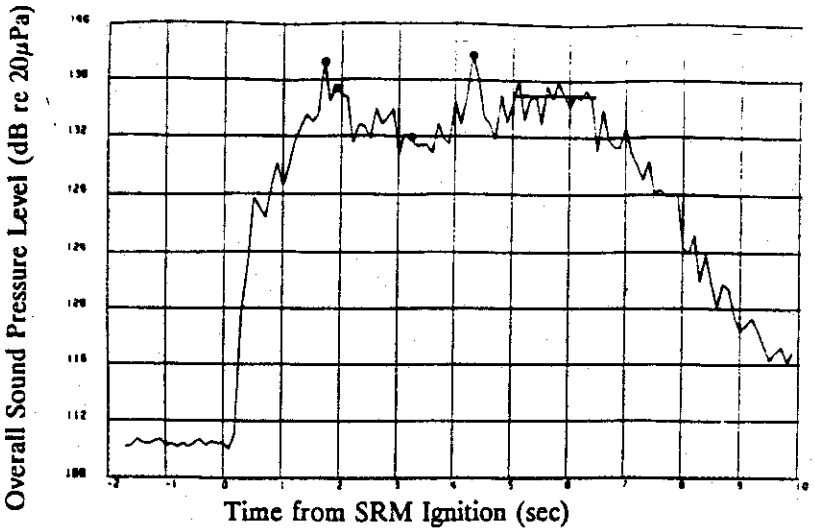

Figure 10. Overall Sound Pressure Level History (Butterworth Plot) of Flight K-4 Measurement 9737 Using an Averaging Time of 0.1 Second, Showing the Effects of Instrumentation System Transients

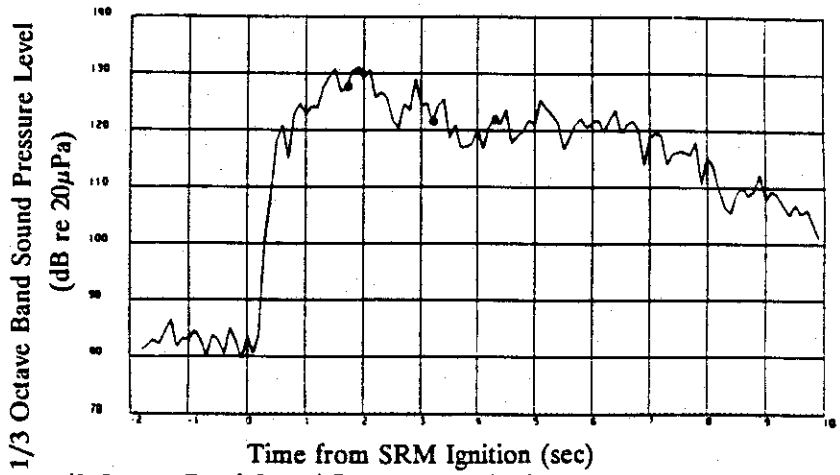

Figure 11. 1/3 Octave Band Sound Pressure Level History (Butterworth Plot) for the Center Frequency of 100 Hz of Flight K-4 Measurement 9737 Using an Averaging Time of 0.1 Second, Showing No Effects of Instrumentation System Transients

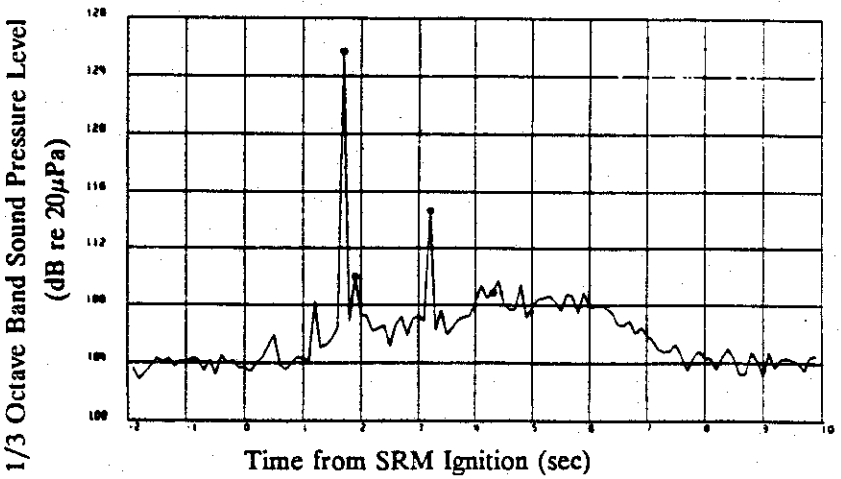

Figure 12. 1/3 Octave Band Sound Pressure Level History (Butterworth Plot) for the Center Frequency of 2.5kHz of Flight K-4 Measurement 9737 Using an Averaging Time of 0.1 Second, Showing the Effects of Instrumentation System Transients and the Background Noise Floor

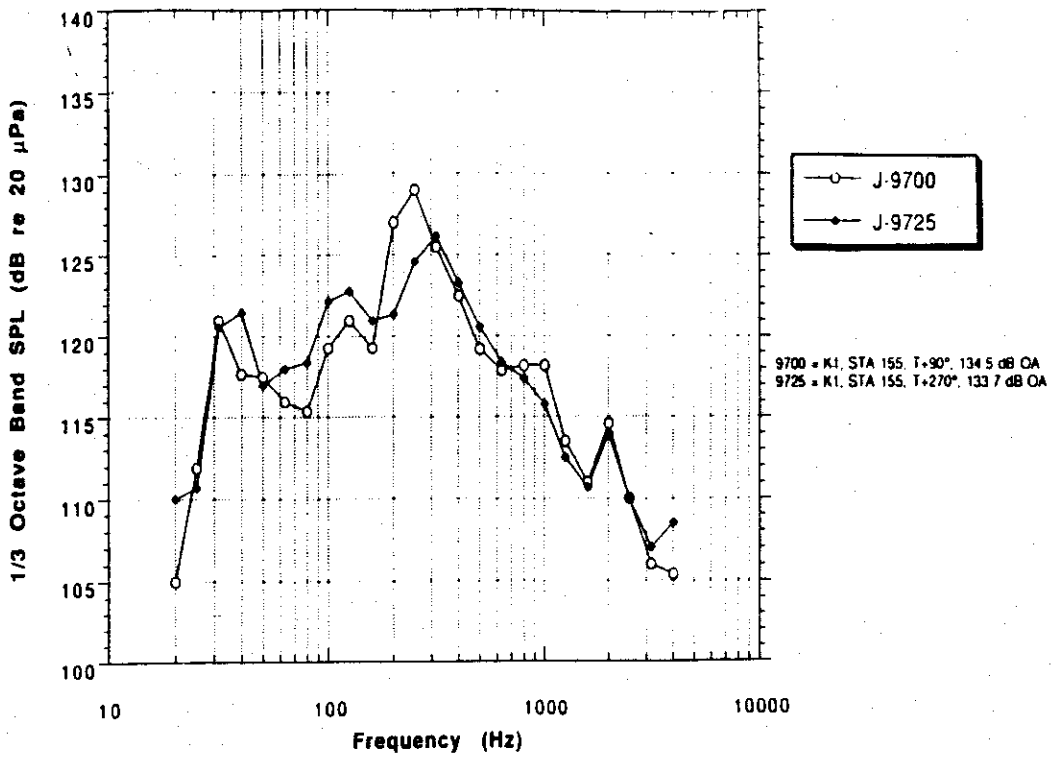

Figure 13. Maximax Acoustic Spectra for Flight K-1 Internal Payload Fairing Measurements During Liftoff

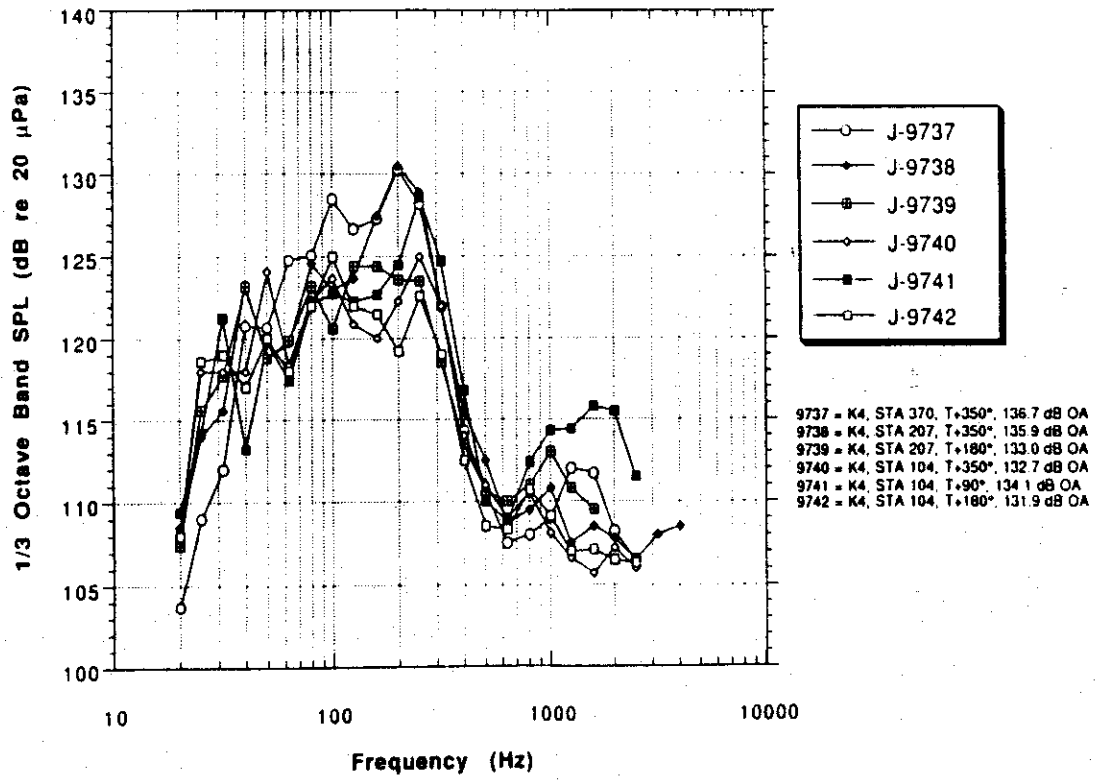

Figure 14. Maximax Acoustic Spectra for Flight K-4 Internal Payload Fairing Measurements During Liftoff

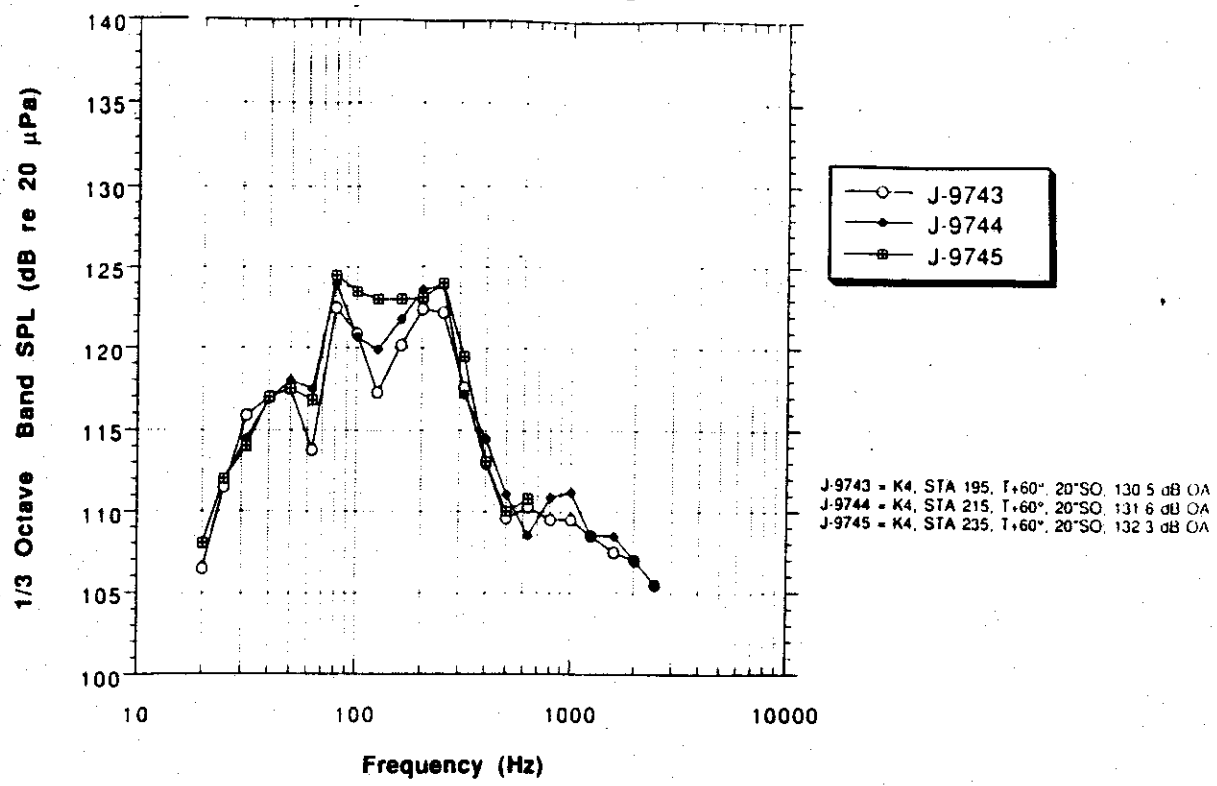

Figure 15. Maximax Acoustic Spectra for Flight K-4 Internal Payload Fairing Measurements Made on 20-Inch Standoffs During Liftoff

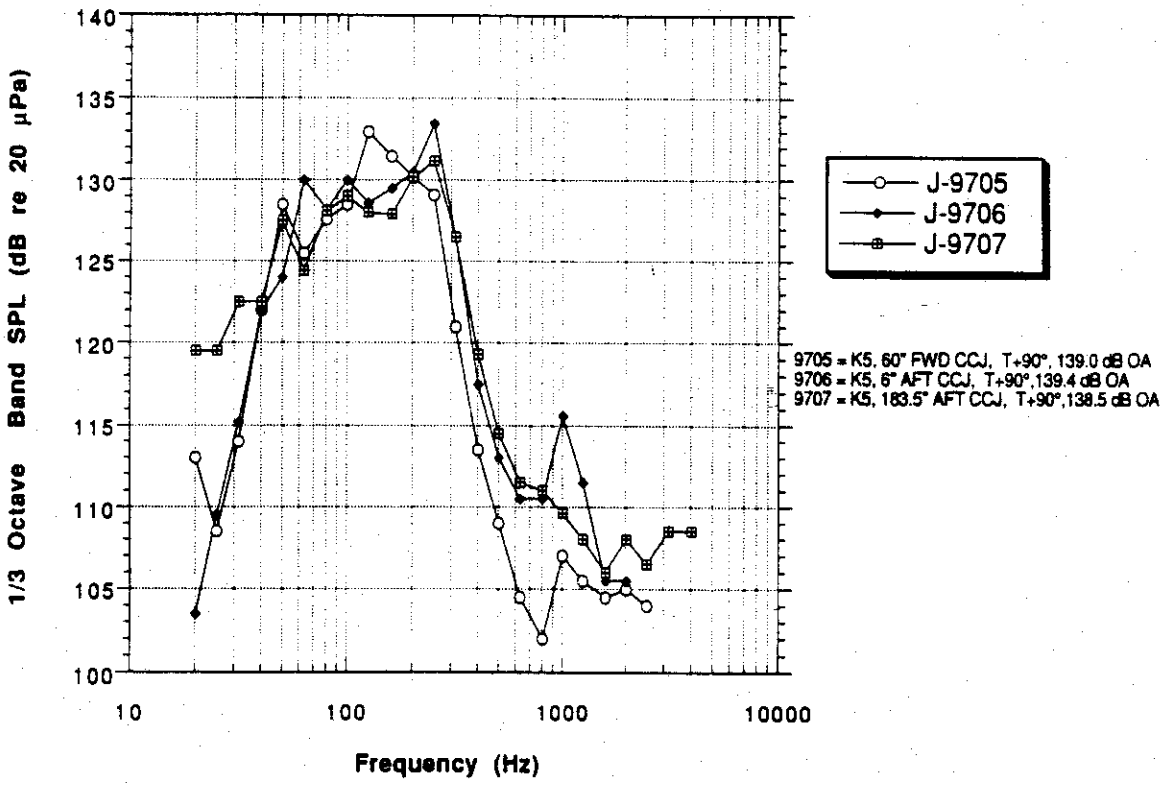

Figure 16. Maximax Acoustic Spectra for Flight K-5 Internal Payload Fairing Measurements During Liftoff

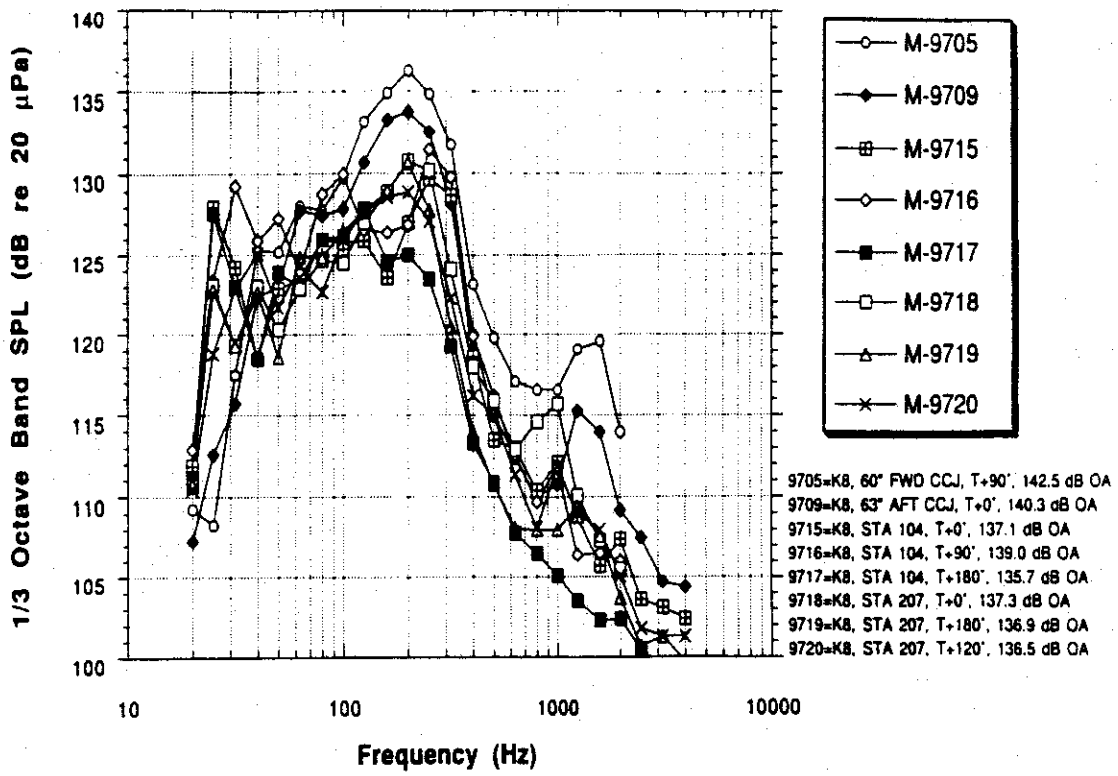

Figure 17. Maximax Acoustic Spectra for Flight K-8 Internal Payload Fairing Measurements During Liftoff

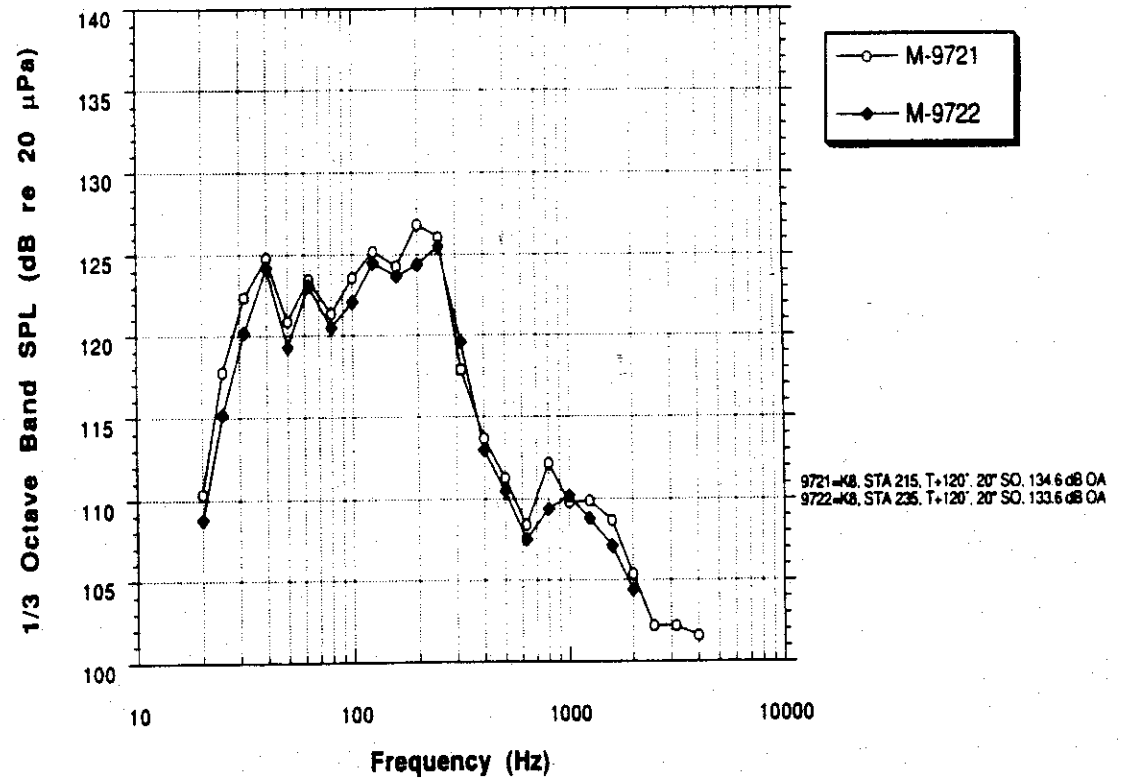

Figure 18. Maximax Acoustic Spectra for Flight K-8 Internal Payload Fairing Measurements Made on 20-Inch Standoffs During Liftoff

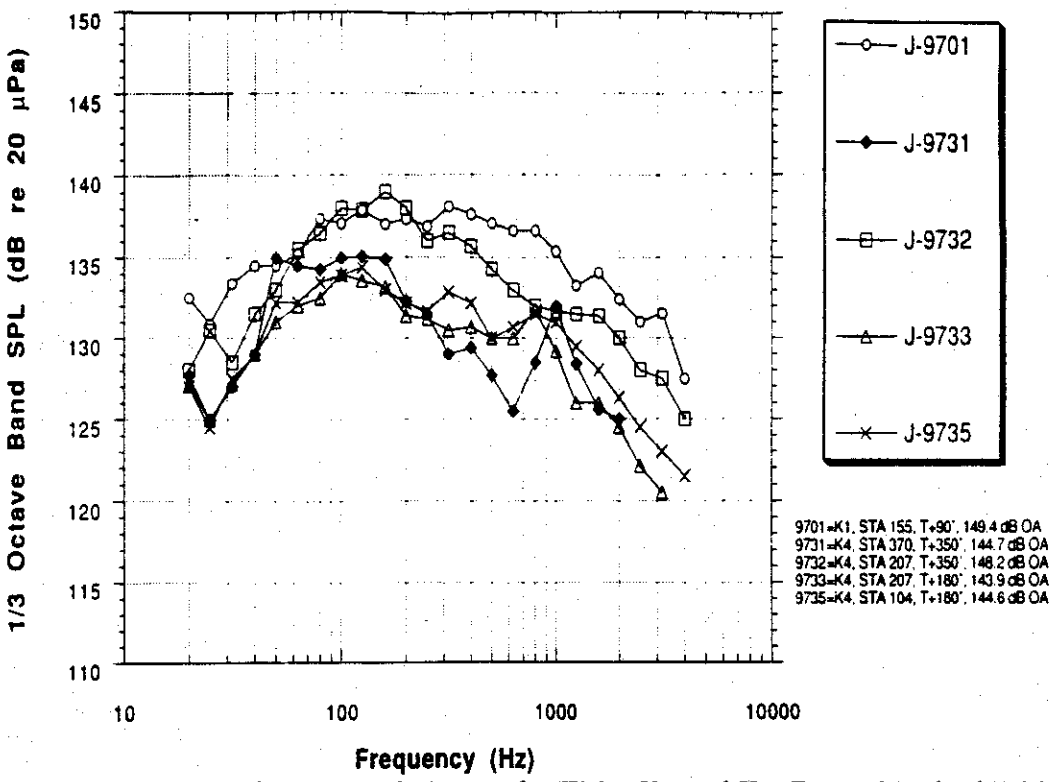

Figure 19. Maximax Acoustic Spectra for Flights K-1 and K-4 External Payload Fairing Measurements During Liftoff

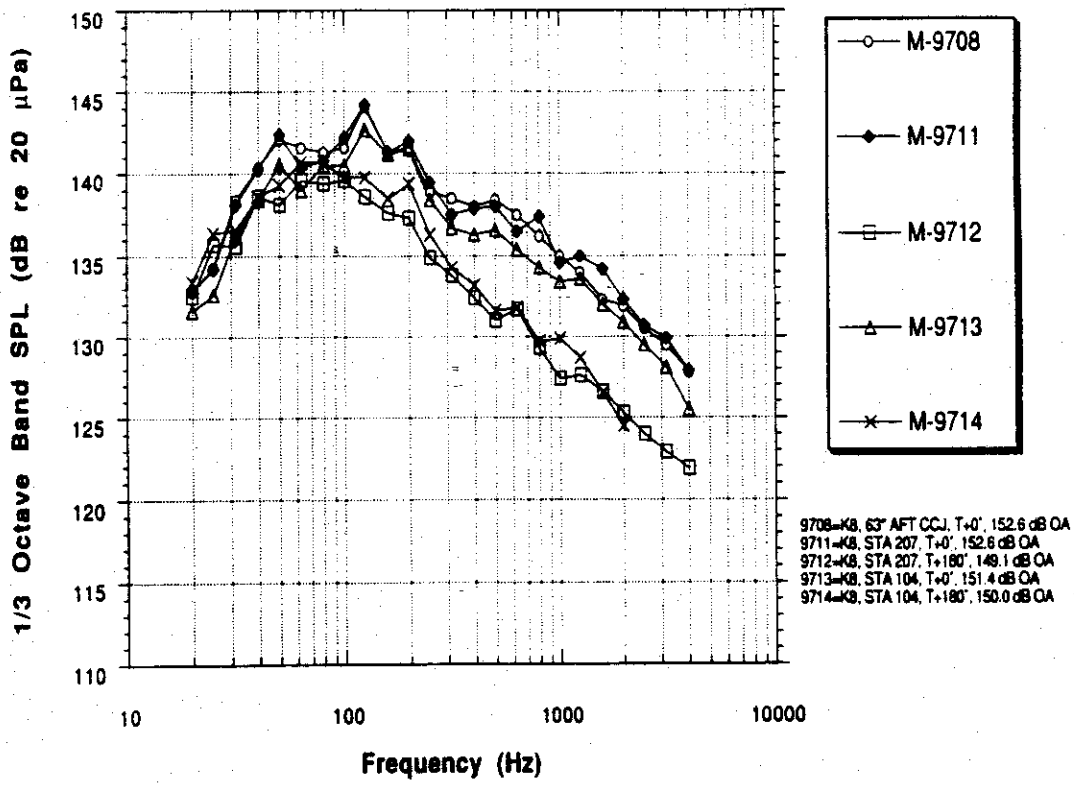

Figure 20. Maximax Acoustic Spectra for Flight K-8 External Payload Fairing Measurements During Liftoff

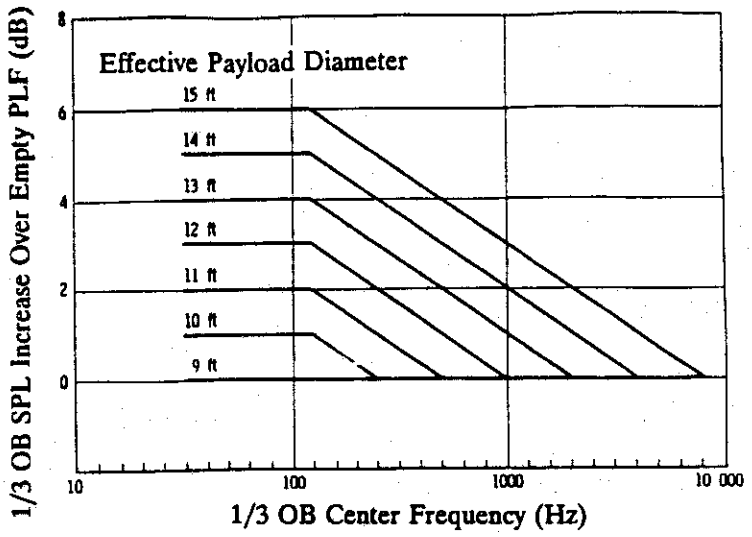

Figure 21. Fill Factor Adjustments to Acoustic Spectra for Shuttle Payloads Based on Effective Payload Diameter (Reference 11)

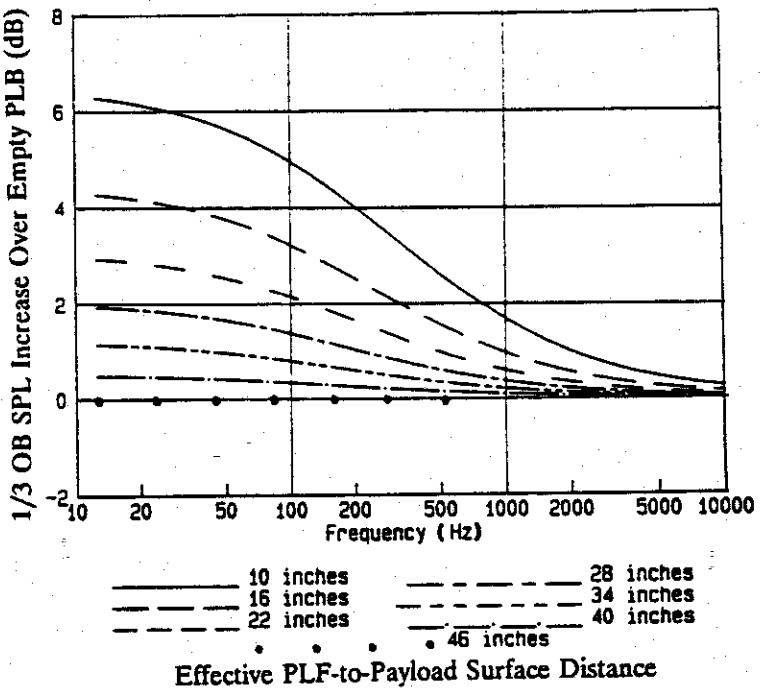

Figure 22. Fill Factor Adjustments to Acoustic Spectra for Expendable Launch Vehicle Payloads Based on Effective Distance from Payload Fairing to Payload Surface (Reference 12)

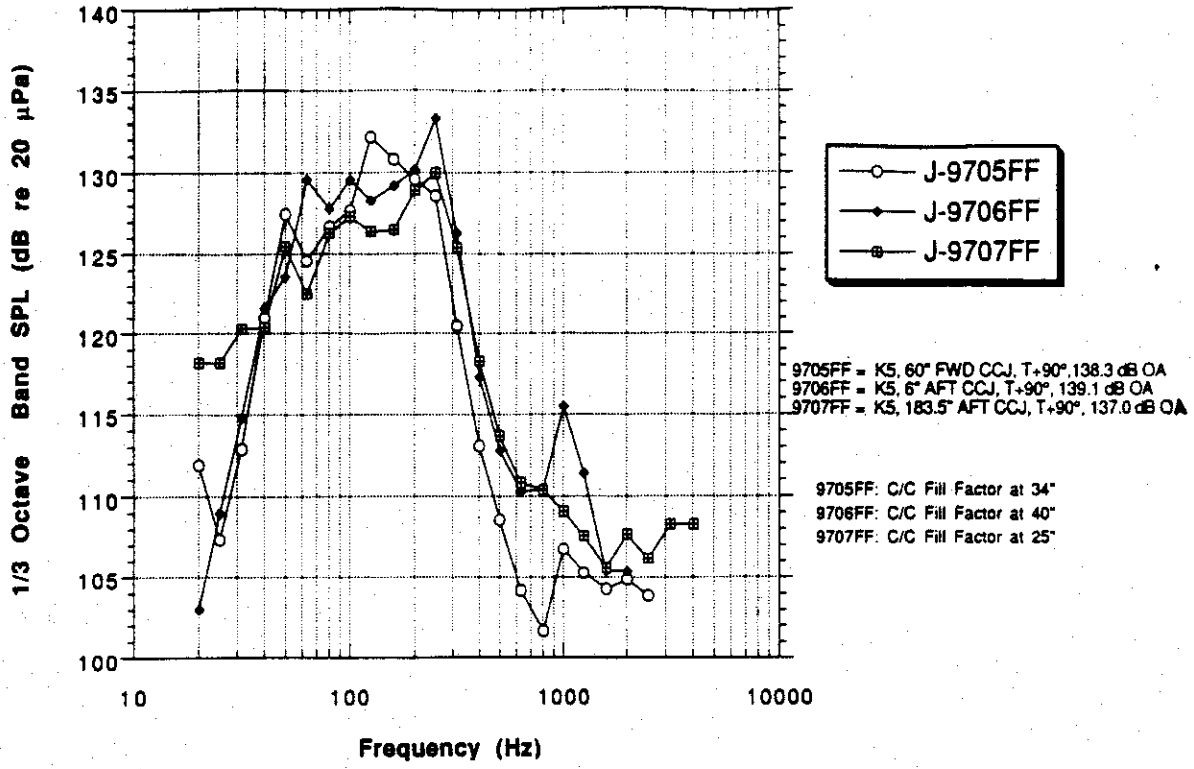

Figure 23. Inverse Fill Factor-Adjusted Maximax Acoustic Spectra for Flight K-5 Internal Payload Fairing Measurements During Liftoff

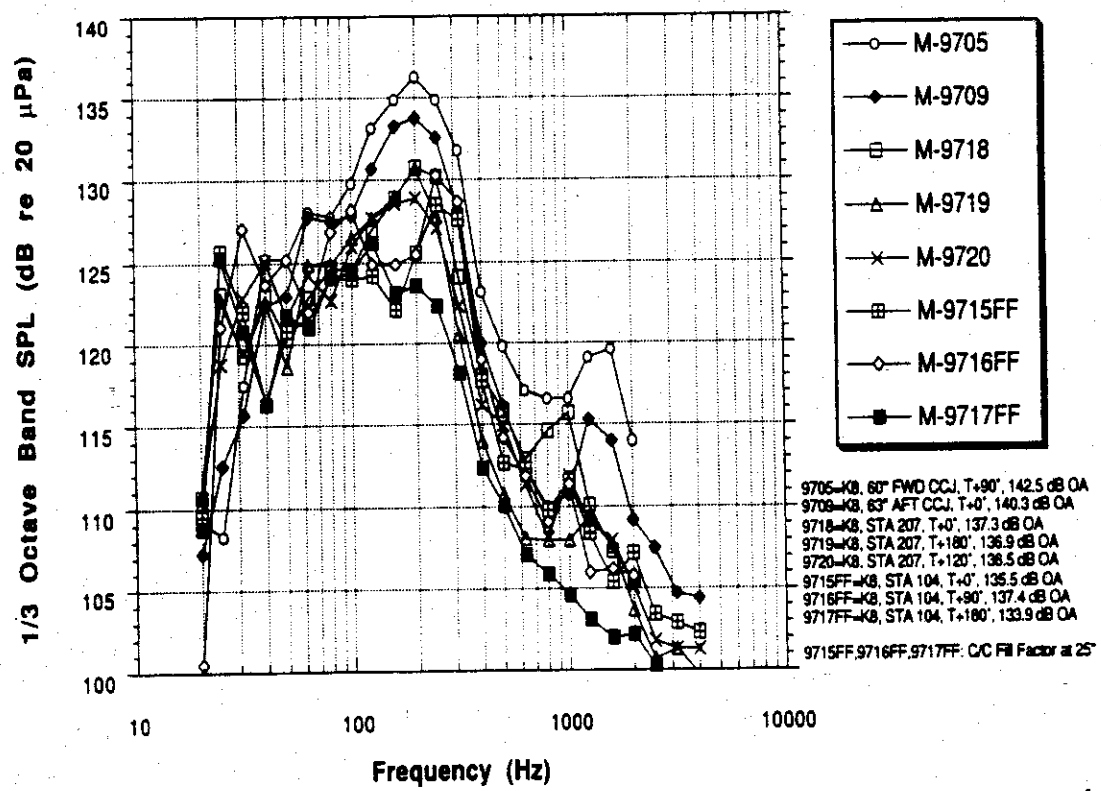

Figure 24. Inverse Fill Factor-Adjusted Maximax Acoustic Spectra for Flight K-8 Internal Payload Fairing Measurements During Liftoff

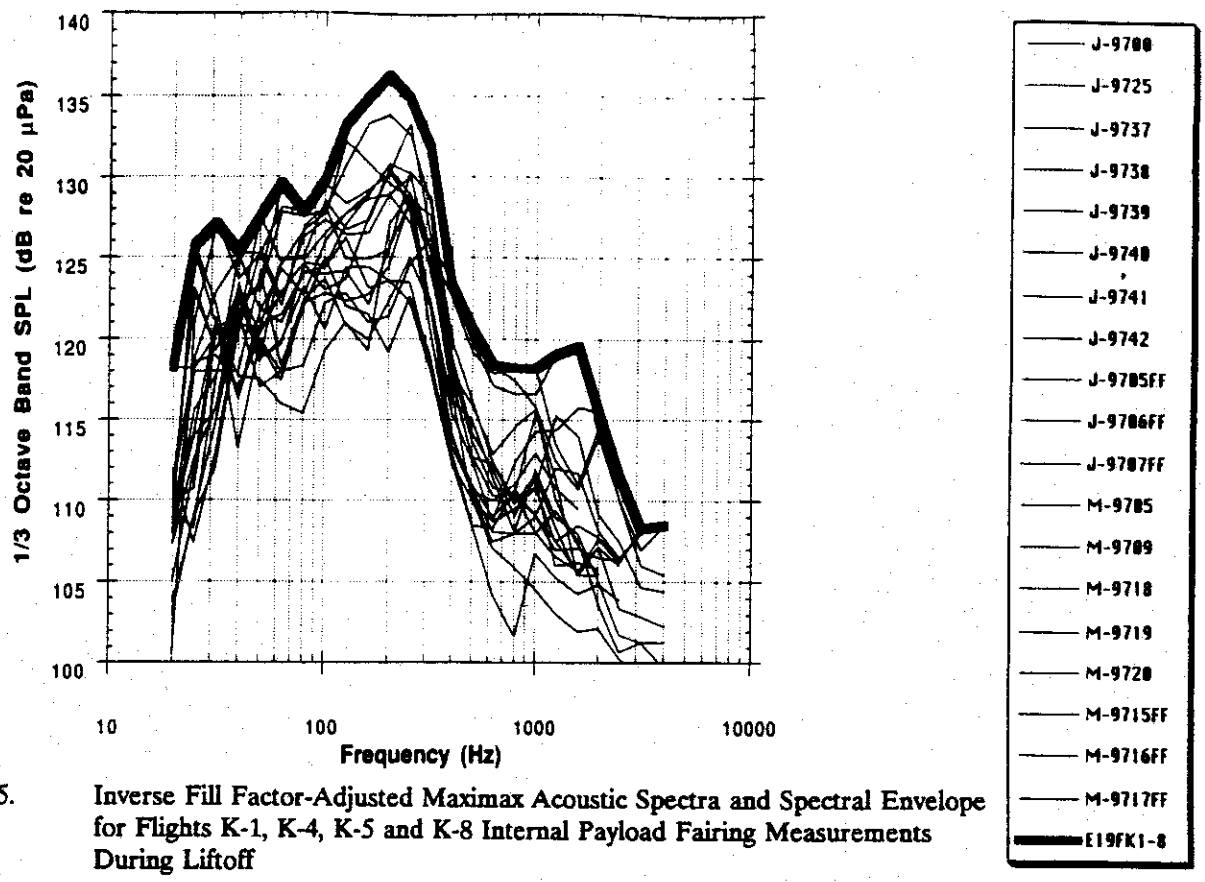

Figure 25. Inverse Fill Factor-Adjusted Maximax Acoustic Spectra and Spectral Envelope for Flights K-1, K-4, K-5 and K-8 Internal Payload Fairing Measurements During Liftoff

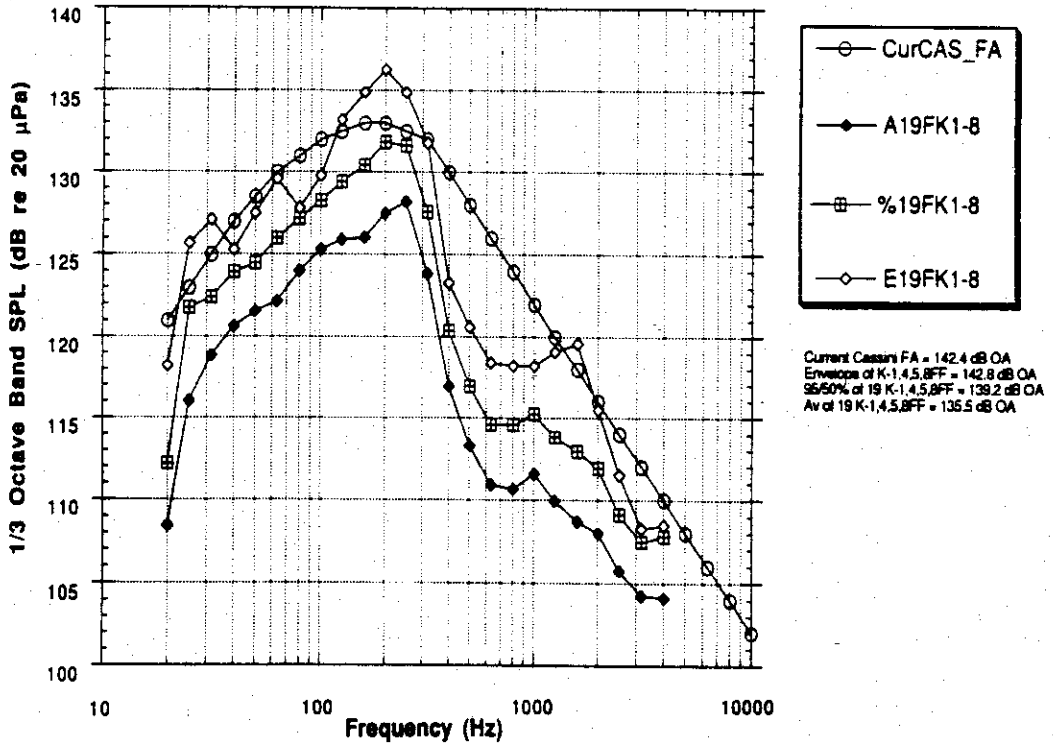

Figure 26. Comparison of Mean and 95/50% Criteria, Based on 19 Inverse Fill Factor-Adjusted Maximax Acoustic Spectra for Flights K-1, K-4, K-5 and K-8 Internal Payload Fairing Measurements, with Spectral Envelope and Current Cassini Flight Acceptance Criteria

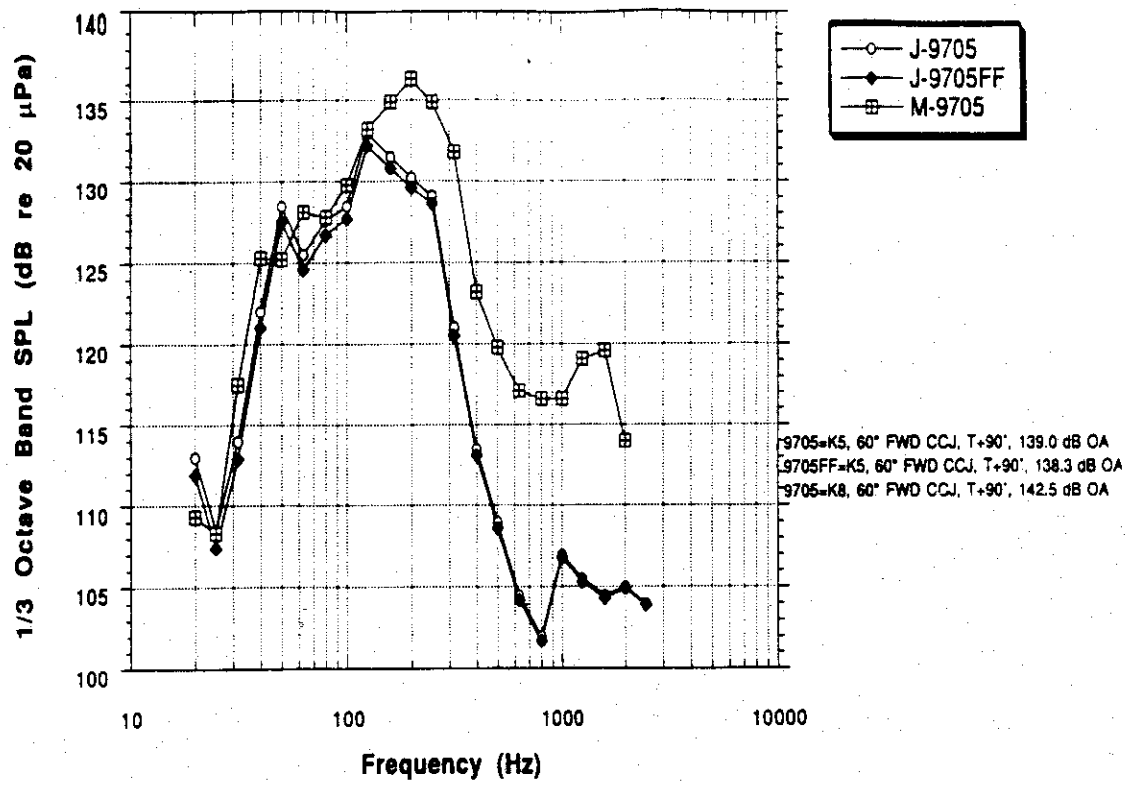

Figure 27. Comparison of Maximax Acoustic Spectra for Measurement 9705 During Liftoff of Flights K-5 and K-8

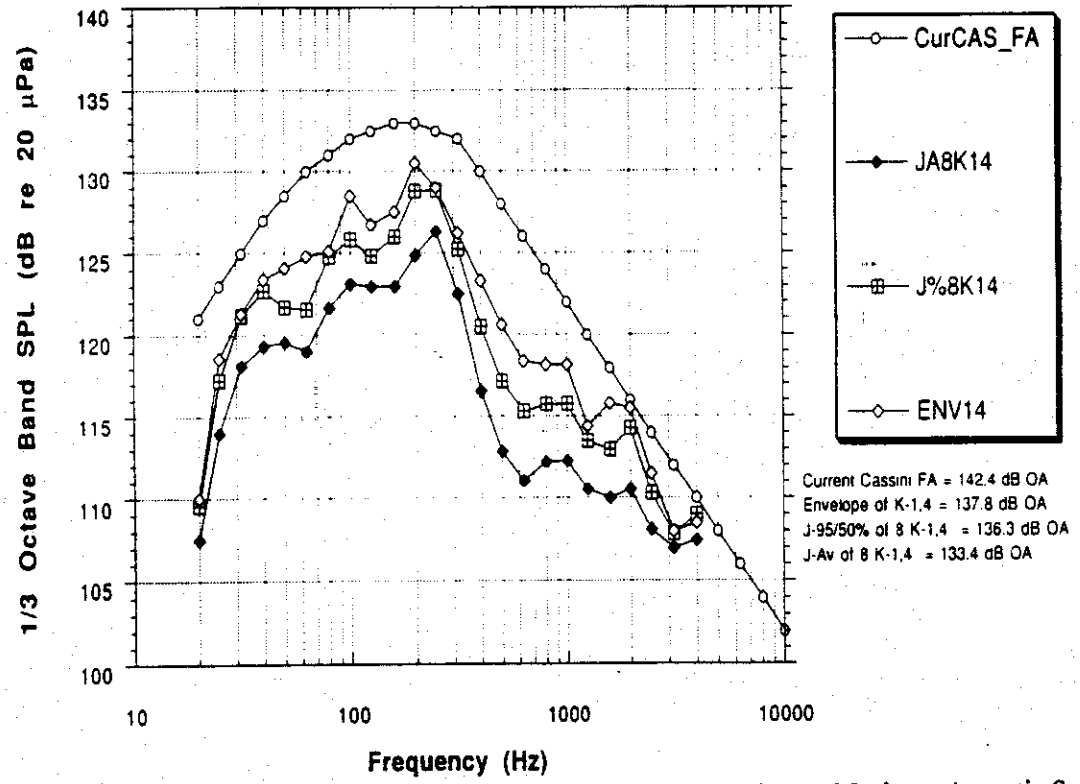

Figure 28. Comparison of Mean and 95/50% Criteria, Based on 8 Maximax Acoustic Spectra for Flight K-1 and K-4 Internal Payload Fairing Measurements, with Spectral Envelope and Current Cassini Flight Acceptance Criteria

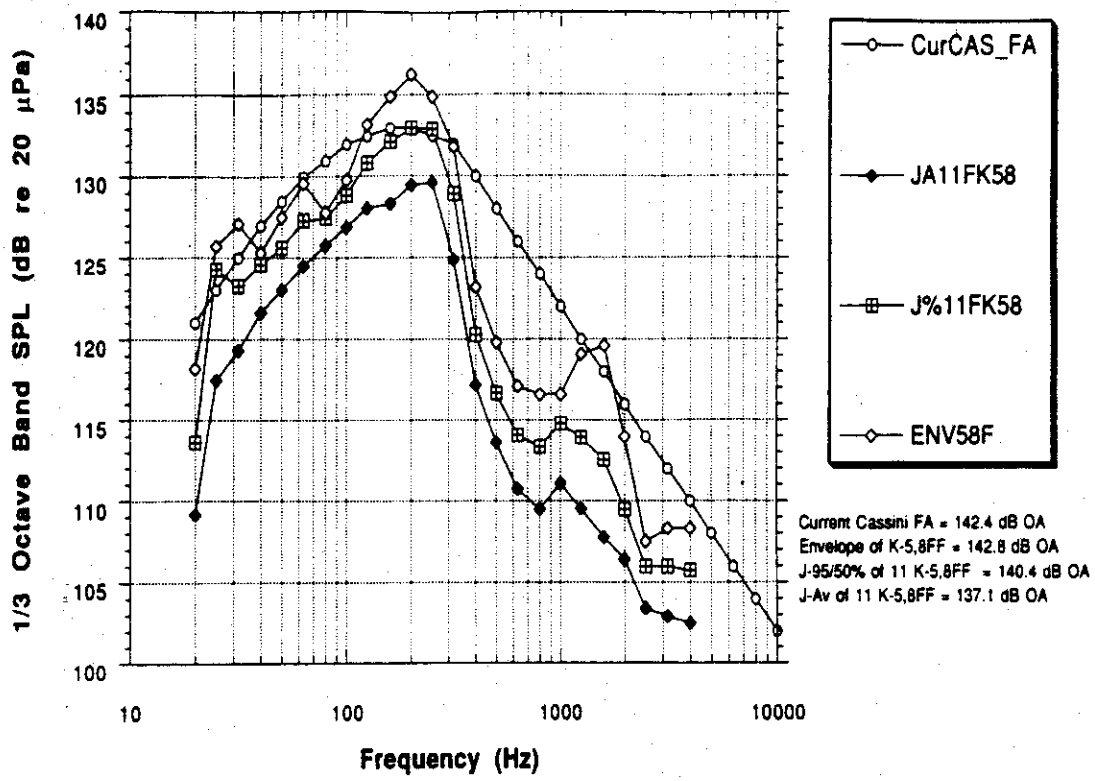

Figure 29. Comparison of Mean and 95/50% Criteria, Based on 11 Inverse Fill Factor-Adjusted Maximax Acoustic Spectra for Flight K-5 and K-8 Internal Payload Fairing Measurements, with Spectral Envelope and Current Cassini Flight Acceptance Criteria

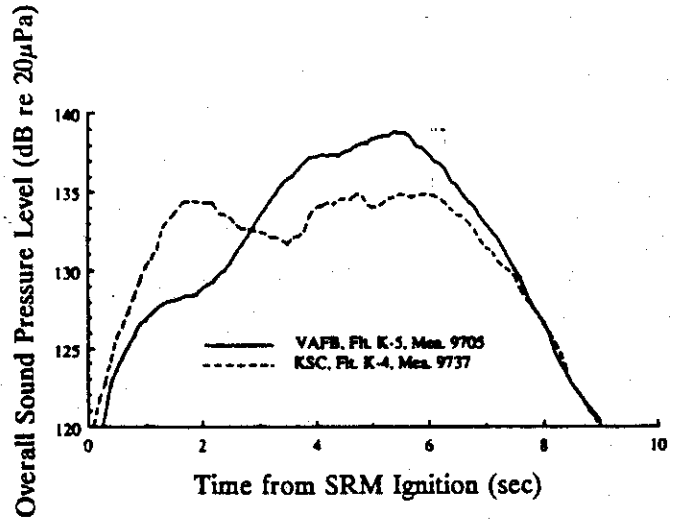

Figure 30. Comparison of Overall Sound Pressure Level Histories Between Internal Payload Fairing Acoustic Measurements During Titan IV Liftoff from the Eastern and Western Test Ranges Using Running Linear Averaging with an Averaging Time of 1 Second (Reference 10)

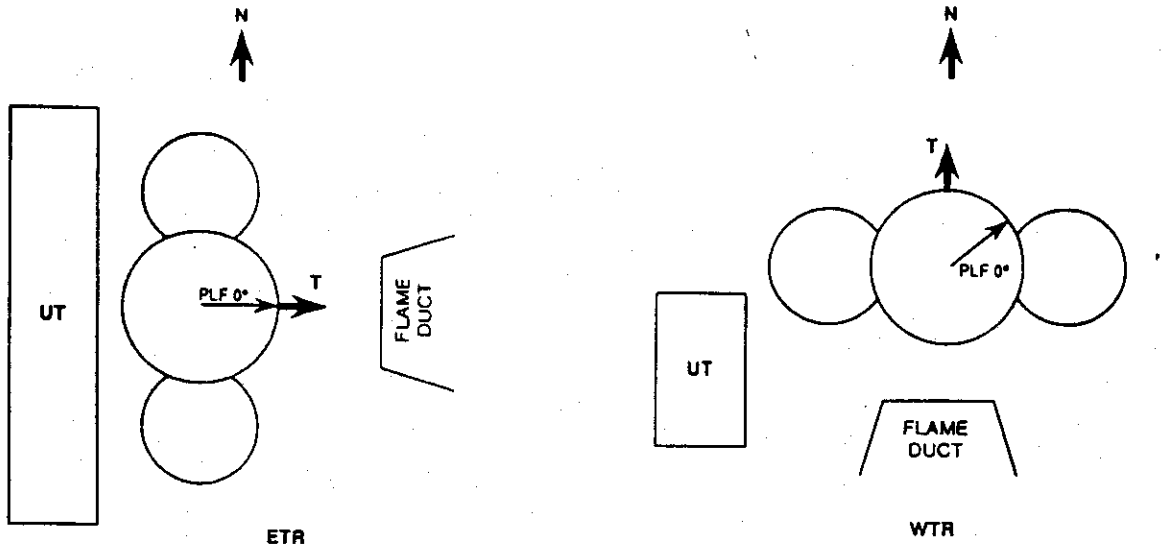

Figure 31. Comparison of Titan IV Launch Pad Configurations Between the Eastern and Western Test Ranges

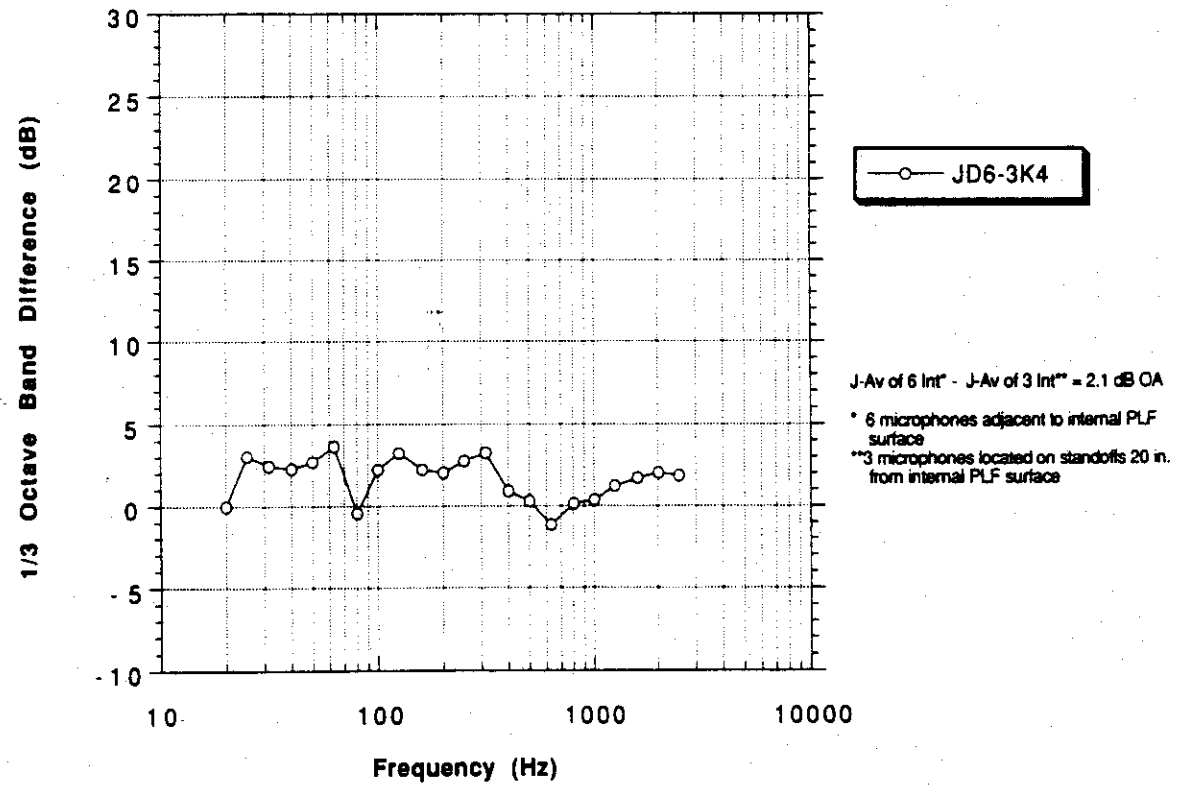

Figure 32. Differences Between Averages of Maximax Acoustic Spectra for the 6 Internal Measurements at the Payload Fairing Surface and the 3 Internal Measurements on 20-Inch Standoffs for Flight K-4 Liftoff

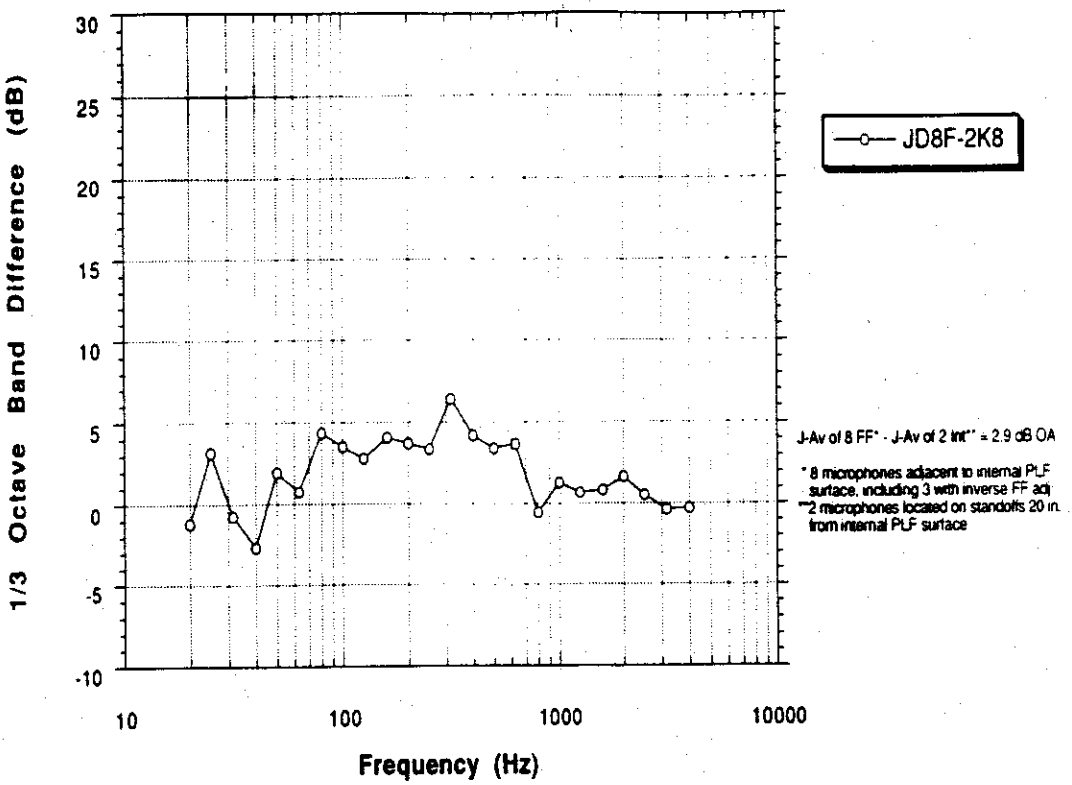

Figure 33. Differences Between Averages of Inverse Fill Factor-Adjusted Maximax Acoustic Spectra for the 8 Internal Measurements at the Payload Fairing Surface and the 2 Internal Measurements on 20-Inch Standoffs for Flight K-8 Liftoff

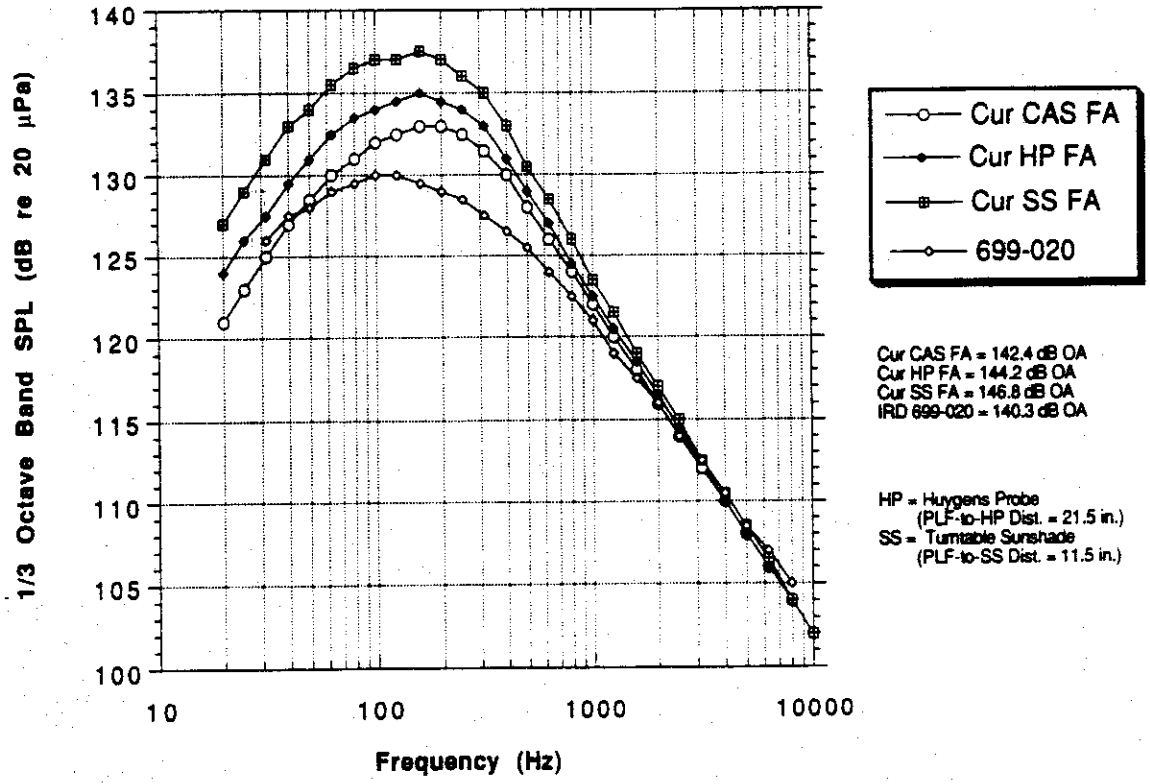

Figure 34. Comparison of Current Flight Acceptance Acoustic Criteria for the Basic Cassini Spacecraft, the Huygens Probe and the Turntable Sunshade

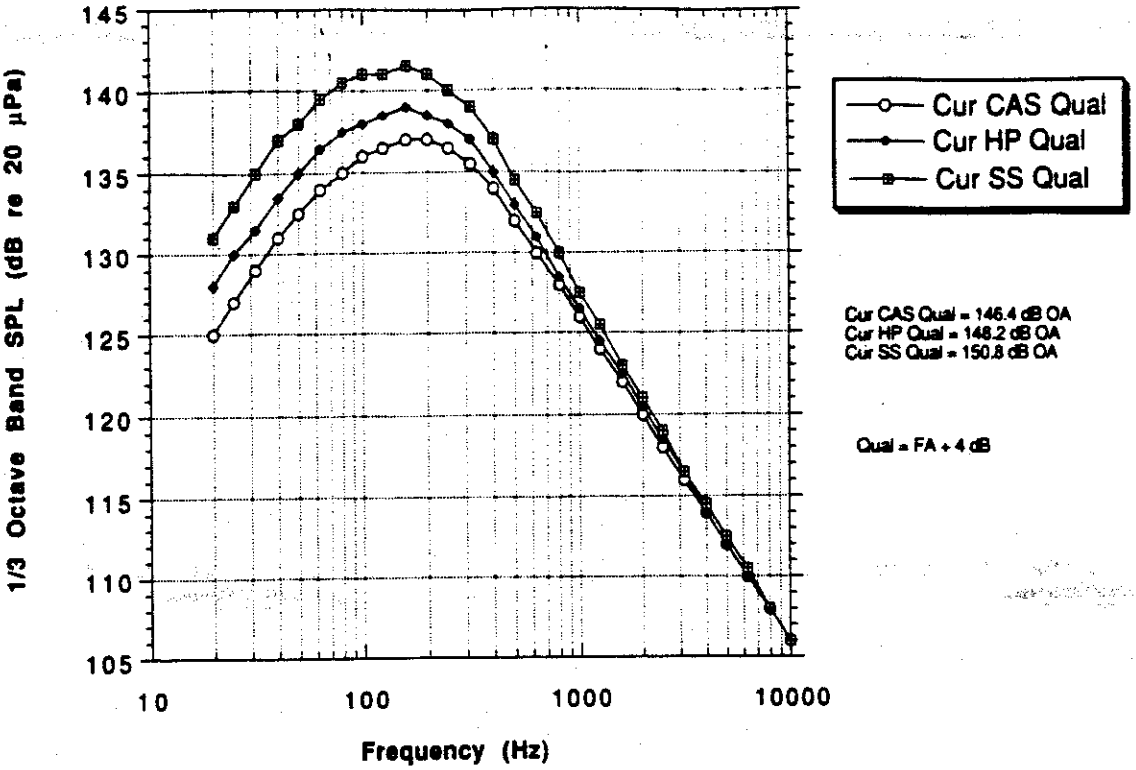

Figure 35. Current Design and Qualification Acoustic Criteria for the Basic Cassini Spacecraft, the Huygens Probe and the Turntable Sunshade